REDOX PHOTOCHEMISTRY OF OXIDATIVELY

MODIFIED NUCLEOBASES

by

Xibo Li

A dissertation submitted to the faculty of
The University of Utah
in partial fulfillment of the requirements for the degree of

Doctor of Philosophy

Department of Chemistry

The University of Utah

August 2015

The University of Utah Graduate School

STATEMENT OF DISSERTATION APPROVAL

The dissertation of   **Xibo Li**

has been approved by the following supervisory committee members:

Cynthia J. Burrows	, Chair	**3/26/2015**
		Date Approved
Darrell R. Davis	, Member	**3/26/2015**
		Date Approved
Janis Louie	, Member	**3/26/2015**
		Date Approved
C. Dale Poulter	, Member	**3/26/2015**
		Date Approved
Matthew S. Sigman	, Member	**3/26/2015**
		Date Approved

and by   **Cynthia J. Burrows**   , Chair/Dean of

the Department/College/School of   **Chemistry**

and by David B. Kieda, Dean of The Graduate School.

ABSTRACT

Present-day organisms recruit flavin as a redox cofactor for various metabolic transformations. In present-day metabolism, it is biosynthesized via several enzyme-catalyzed steps from guanosine triphosphate (GTP). It is hypothesized that life originated from RNA on the primordial Earth. If this hypothesis holds true for the so-called "RNA World", there should be a counterpart for the most critical molecules we encounter in present-day biology. Thus, we asked what molecule(s) could predate a present-day flavin to support primitive metabolisms. We also try to answer why Mother Nature selected flavin over many other potential candidate molecules from the photophysical perspective.

Toward these goals, we studied the photoredox properties of some oxidatively modified nucleobases. Specifically, we studied 5-hydroxypyrimidine and its ability to photochemically repair a thymine dimer in double stranded DNA. It was found that the repair rate is dependent on many factors, including pH, base pairing, and its position relative to the thymine dimer. For these candidate molecules to carry out functions similar to what flavin does in photolyase, we investigated the concept of noncovalent interaction between a free 8-oxoguanine as a flavin mimic and an abasic site in double stranded DNA as a ribozyme model, and found that it can accelerate thymine dimer repair. Not surprisingly, noncovalent interactions that bind the photocatalyst to the DNA duplex can accelerate thymine dimer repair compared to a bimolecular reaction. However, the repair efficiency is still lower than that of photolyase. We thus studied the photophysical proper-

ties of one candidate molecule, 8-oxoguanine. To study the excited-state decay of 8-oxoguanine in the presence of base stacking, we optimized a synthetic methodology to prepare an 8-oxoguanine-containing dinucleotide. Pump-probe experiments performed by collaborators demonstrated that a deactivation channel through charge-transfer state formation between 8-oxoguanine and adenine exists in the dinucleotide, and potentially also exists in oligonucleotides. To study 8-oxoguanine excited-state decay in the more relevant double-stranded DNA, we explored various methodologies of circularizing short dsDNA and developed a postsynthetic modification method featuring click chemistry to synthesize a minicircle of DNA. The synthesized minicircle DNA is only two base-pairs long and very stable at room temperature. Through circular dichroism experiments, we found that the conformation of minicircle DNA is not necessarily B-form and is sequence-dependent. Pump-probe experiments were also performed on these molecules.

To the memory of grandpa, LI Bing Xian (1928-2000), and grandma, XU Ren Lan (1930-2014), for their inspiration and selfless love

TABLE OF CONTENTS

CHAPTERS

LIST OF TABLES

LIST OF FIGURES

x

Chart

Scheme

LIST OF ABBREVIATIONS

A	adenosine
ACN	acetonitrile
AP	abasic site
C	cytidine
CD	circular dichroism
CPD	cyclobutane pyrimidine dimer
CT	charge transfer
CuAAC	copper-catalyzed alkyne-azide cycloaddition reaction
D	2-amino dA
DCI	4, 5-dicyanoimidazole
DCM	dichloromethane
DMAP	4-dimethylaminopyridine
DMF	dimethylformamide
DMSO	dimethylsulfoxide
DMT	dimethoxytrityl
dsDNA	double stranded DNA
dO	8-oxo-7,8-dihydro-2'-deoxyguanosine
GSB	ground state bleaching

EDTA	ethylenediaminetetraacetic acid
EET	excess electron transfer
ESA	excited state absorption
ET	electron transfer
F	tetrahydrofuran analog
FAD	flavin adenine dinucleotide (oxidized form)
FADH$_2$	flavin adenine dinucleotide (reduced form)
FTIR	fourier transform infrared spectroscopy
G	guanosine
5-HC	5-hydoxycytosine
HPLC	high performance liquid chromatography
HRMS	high resolution mass spectrometry
5-HU	5-hydroxyuracil
IC	internal conversion
IR	infrared
ITC	isothermal calorimetry
MES	2-(N-morpholino)ethane sulfonic acid
MTHF	methylenetetrahydrofolate
MS	mass spectrometry
NAD+	nicotinamide adenine dinucleotide (oxidized form)
NADH	nicotinamide adenine dinucleotide (reduced form)
NHE	normal hydrogen electrode
O	8-oxo-7,8-dihydroguanosine

PCET	proton-coupled electron transfer
PEG	polyethylene glycol
R	8-amino dG
ROS	reactive oxygen species
RP-HPLC	reversed phase high performance liquid chromatography
ssDNA	single stranded DNA
T	thymidine
TBTA	tris[(1-benzyl-1H-1,2,3-triazol-4-yl)methyl]amine
TEAA	triethylammonium acetate
TRIR	femtosecond time-resolved infrared
T=T	[*cis, syn*] thymine dimer
U	uridine
UPLC	ultra performance liquid chromatography
UV	ultraviolet
Vis	visible

ACKNOWLEDGEMENTS

A dozen years have passed since I first started graduate school. It has been a long journey, with lots of ups and downs, which I consider an invaluable treasure for my life. I am fortunate enough to have so many people who have helped me to the finish line. Without them, I wouldn't be where I am today.

First and foremost, I gratefully acknowledge my advisor Dr. Cynthia J. Burrows for giving me the opportunity to finish graduate school, and for providing me with the training and tools necessary to succeed in my future career. I appreciate the help and support she gave me when I was having a difficult time in the spring of 2011.

I am very thankful for the support of my dissertation committee: Dr. Darrell R. Davis, Dr. Janis Louie, Dr. C. Dale Poulter, and Dr. Matthew S. Sigman. It has been an honor to develop as a scientist under their guidance.

I would like to acknowledge our collaborator Dr. Bern Kohler and his group members, especially Dr. Yuyuan Zhang and Ashley Beckstead at Montana State University. With their wisdom and expertise on femtosecond transient absorption spectroscopy, our constructive collaboration has produced several papers.

I feel enormously lucky to have worked with so many friendly, supportive, and inspiring Burrows group members, past and present. Former Burrows group member Dr. Khiem V. Nguyen patiently showed me the ropes. Dr. Aaron M. Fleming has taught me many useful tips and provided me with plenty of helpful advice.

In my early graduate school years, several other former advisors have helped and trained me on various aspects. They are Prof. Qinhua Song (USTC), the late Prof. Lawrence M. Sayre (CWRU), Prof. Irene Lee (CWRU), and Prof. Jon D. Rainier. I also need to thank them and their awesome group members.

I thank my family for their constant support and love, despite the 6,175 miles between us. My parents frequently fly to Salt Lake City to help me take care of my two little kids. I really enjoy the time with them. Their support, sacrifice, and understanding over the years mean a lot to me. I am thankful to my parents-in-law for their support. I am also thankful to Danni and Danyu. They are the meaning of my life. I thank them for bringing joy and happiness to our family.

Most especially, I thank my wife, Aixiang Liu, whose constant love and support has allowed me to endure the difficult moments and rejoice in the happy moments. I am grateful for her sacrifices to accompany me to pursue my education. I dedicate all of my work, past and future, to her.

CHAPTER 1

INTRODUCTION

Every bit of information about modern life is encompassed by the central dogma of molecular biology. It often seems that the life cycle relies on DNA, while RNA only plays a subordinating role. However, more and more evidence has suggested that RNA is indispensable, especially when we debate whether life could begin with RNA. Critical to the RNA world hypothesis (*1*) is, besides RNA's information processing function, its capability of metabolic transformations as diverse as protein-based enzymes in order for biology to emerge from chemistry in the primordial soup (Figure 1.1). Since the finding of the first natural catalytic RNA by Altman (*2*) and Cech (*3*), miscellaneous evidence has been found to support RNA's catalytic role. Among them are nucleotide synthesis (*4*), aminoacylation (*5, 6, 7*), RNA polymerization (*8, 9*), phosphorylation (*10*), proteolysis (*11*), ligation (*12, 13*), peptide bond formation (*14, 15*), hydrolysis, and carbon-carbon bond formation (*16, 17*). The finding of ribosomal RNA catalyzing peptide bond formation in a ribosome (*15*) is often hailed as the "smoking gun" evidence in support of the RNA world hypothesis. Assuming the RNA world is established, the RNA-based genome can (*18*) and must continuously evolve over time in response to various environmental pressures in order to survive.

Unfortunately, fossil records about the RNA world genome and its "proteome" have
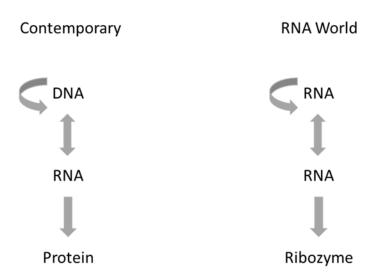
Figure 1.1 Central dogma of the contemporary and the hypothesized RNA world.

disappeared in the long history of the Earth. We could not know exactly what they looked like, but could reinvent them (*19*) from known facts. Take the cellular repair machinery; for example, present-day nucleobases are suffering constant assault from UV irradiation leading to photodamage, which left without repair could have serious biological consequences (*20*). The damage could, however, be mitigated and repaired by modern repair machinery (*21, 22, 23, 24*). This UV irradiation damage could have been much stronger on primordial earth, presumably due to the lack of enough ozone protection, especially before the "Great Oxidation Event" (*25*) when oxygen levels are thought to start to rise due to the appearance of photosynthetic species. Primitive RNA genomes may be especially sensitive to these photodamages as high error rates could hamper genetic information passage from one generation to the next. Thus, the primordial ribozyme must also evolve to repair these photodamages. In present-day lower organisms, the photodamage is repaired by photolyase facilitated by a redox cofactor flavin, which functions as the electron donor due to its low redox potential (*24*). Analogously, the primitive ribozyme may also need to recruit a redox cofactor because the four canonical nucleobases are not redox active (*26*). Therefore, a redox molecule may predate present-day flavin before modern mechanisms could biosynthesize in a series of coordinated steps (*27*). Many researchers have speculated about the nature of early coenzymes and suggested their origin from RNA bases (*28, 29*).

8-Oxoguanine as flavin mimic? Consideration of its excited-state dynamics

In our continued interest in searching for a flavin surrogate, a common oxidation product of guanine, 8-oxo-7,8-dihydro-2'-deoxyguanine (O), caught our attention.

Remarkably, it exhibits quite similar reactions to that of flavin (*30, 31, 32, 33, 34, 35, 36, 37, 38, 39, 40*). While there are considerable parallels between the chemistry of O and flavin, there are differences as well (Figure 1.2). For example, the oxidized flavin is stable while oxidized O, O^{ox}, is not. O^{ox} can undergo nucleophilic addition at C5 leading to rearrangement to spiroiminodihydantoin (*39, 41, 42, 43*). On the contrary, the reduced form of flavin is unstable in air while O is stable (*44*). In modern biology, riboflavin is biosynthesized from GTP, first by a ring-opening reaction to form the formamidopyrimidine (Fapy-G). Interestingly, ionizing radiation of G can generate both Fapy-G and O, and these reactions are also feasible under UV irradiation and Fenton reaction conditions (*45*).

Recently, the Burrows laboratory demonstrated that O can also repair a thymine dimer in DNA by the same mechanism as flavin in photolyase-catalyzed thymine dimer repair (*46, 47*) though with a lower quantum yield. On the contrary, in photolyase-catalyzed thymine dimer repair reaction, the quantum yield almost achieves unity (*24, 48*). Two competing pathways may contribute to the observed quantum yield difference: (1) the long excited-state lifetime of flavin (1.3 ns) vs. fast forward electron transfer (ET) to thymine dimer (250 ps), and (2) futile, slow back ET from thymine dimer radical anion to flavin radical (2.4 ns) vs. fast second bond C_6-$C_{6'}$ cleavage (90 ps) (Figure 1.3). All of these factors favor an extremely efficient thymine dimer repair reaction. In the chemical model of thymine dimer repair systems, however, the quantum yields are significantly low (*49, 50, 51*), even for covalently linked flavin model systems (*52, 53*). Femtosecond-resolved transient fluorescence spectroscopy shows that the excited-state of flavin in the model system (*54*) decays significantly faster (5.8 ps) than in photolyase (1.3 ns) (*48*),

Figure 1.2 Structure similarity of O and flavin and their oxidized forms.
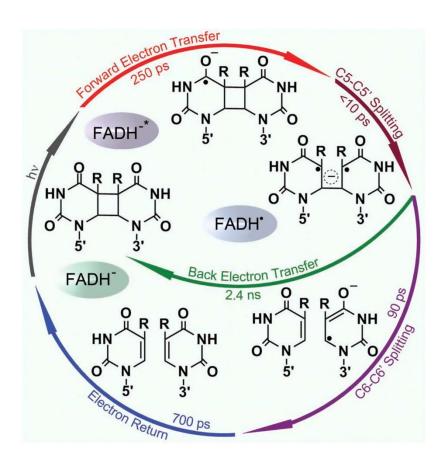
Figure 1.3 Complete photocycle of CPD repair by photolyase. *Reprinted with permission from Liu et al. (48). Copyright 2011 National Academy of Sciences, USA.*

indicating the more flexible the environment, the shorter the excited-state lifetime of fully reduced flavin (Figure 1.4). Therefore, this ultrafast decay of free flavin may predetermine the low quantum yield of the model system even though it has faster forward ET (79 ps) than in photolyase (250 ps). The small overall quantum yield may also be determined by futile, faster back ET in the model system (95 ps) than in photolyase (2.4 ns), in addition to slower breakage of the second bond in the model system (435 ps) than in photolyase (90 ps).

In DNA, all four canonical bases can convert absorbed light energy into heat within 1 ps (*55*), thus preventing their decomposition at a high energy state. This ultrafast deactivation is probably one of the unique advantages arising from many selection pressures over eons (*56*). Mounting evidence has shown that the excited-state lifetimes of nucleobases are dependent on many factors including base stacking (*57*) and base pairing (*58*). Based on these experiments, we ask the following question: could the low quantum yield of O repairing thymine dimer in a duplex also be due to its short excited-state lifetime? If so, what other factors could affect its excited-state lifetime? Interesting phenomena were observed during the photo-induced thymine dimer repair experiment, in which a higher repair yield was recorded when O base pairs with A vs. C (Figure 1.5) (*46*). A computational study suggested that proton-coupled electron transfer between O and C may shorten its excited-state lifetime and account for the observed repair yield discrepancy (*59*). To address these questions, we will discuss efforts on measuring its excited-state lifetime in various contexts. These studies may pave the road to future direct observations of thymine dimer repair dynamics.
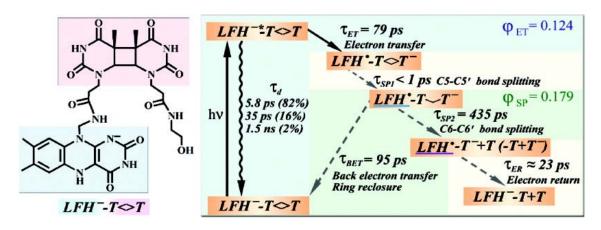
Figure 1.4 Repair scheme of thymine dimer repair by covalently linked flavin. *Reprinted with permission from Kao et al. (54). Copyright 2012 American Chemical Society.*
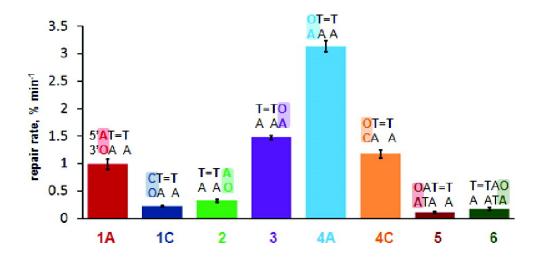
Figure 1.5 Repair rates at 22 °C for various sequence contexts for O and T=T. *Reprinted with permission from Nguyen et al. (46). Copyright 2011 American Chemical Society.*

Continual screening of redox nucleoside

Contemporary genomes use only four canonical bases to store the tens of thousands of genetic information. However, nucleobase modification is ubiquitous and could be found playing various vital functions in all stages of life cycle across all domains of life. Various modified RNA bases would have existed in the RNA world as they still do among various special RNAs and may even have played an important role that could have been lost during the transition from the RNA world to the DNA world. Canonical RNA bases are likely the result of various selection processes (*56, 60*).

In our continued interest in searching for flavin surrogates, we take into consideration the following criteria. First, it should have a long wavelength absorbance, ideally above 300 nm where all canonical bases do not have absorption at all. Thus, the surrogate can take advantage of abundant low energy solar light. Second, it should be a good electron donor. In another word, it should have low redox potential. Third, it should have a long excited-state lifetime. Otherwise, the absorbed energy will be efficiently converted into useless heat and dissipated to the environment.

Compared to canonical pyrimidines, the UV absorption spectroscopy of 5-hydroxy-pyrimidines is red-shifted, though the maximum of the absorption peak is pH-dependent. As with other nucleobase oxidation products, such as O, their redox potentials are much lower than their parent nucleobases. Depending on the oxidant, 5-hydoxypyrimidines can be further oxidized reversibly (*61*) or irreversibly (*62*), suggesting their reasonable stability. Most importantly, the excited-state lifetime of 5-hydroxyuracil is reported to be 1.8 ns in the gas phase (*63*). These embedded characteristics make them ideal candidates as potential photo-redox catalysts (Figure 1.6). Even though it is held that the atmosphere
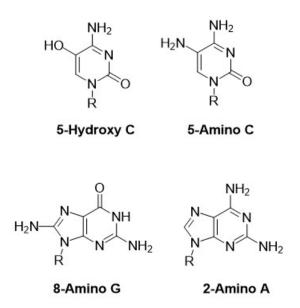
Figure 1.6 Other potential flavin mimic molecules

of primordial earth is mainly reductive, oxidative processes, such as the Fenton reaction, are still possible especially on the "Snowball Earth" (*45*). Thus, 5-hydoxypyrimidines probably existed on the primordial earth. They can still be found in contemporary RNA sequences even though their function is unknown (*61, 64, 65*).

There are many other modified RNA bases that meet the above-mentioned criteria. For example, computational studies suggest 5-aminopyrimidines have red-shifted UV absorption spectra (*66*), low redox potential as with 5-hydroxypyrimidines (*67*), and long gas-phase excited-state lifetime (*63*). Recently, 8-amino dG was computationally suggested to be as active as O (*68*), thus deserving further investigation of its thymine dimer repair ability. 2-Amino-dA has a relatively long gas-phase excited-state lifetime, 6.3 ns (*69*), however, a slightly lower redox potential than G (*70*). It will be interesting to investigate their thymine dimer repair potential as well. This study will answer whether excited-state lifetime can outweigh redox potential. Of course, we should also know their excited-state lifetime in solution phase as it may be quite different from the one reported in the gas phase.

In order for our proposed flavin mimics to function as a primitive coenzyme, the ribozyme must also evolve to utilize it in some way, preferably via noncovalent interaction as in photolyase. There is only one example of flavin usage via covalent linkage to ribozyme (*71, 72*). However, no ribozyme has been found that could use flavin noncovalently. Thus, we designed a model to showcase that noncovalent interaction, mainly hydrogen bonding and van der Waals interactions, between the "ribozyme" and a flavin mimic can efficiently carry out the function.

Conclusion

As was said by Albert Eschenmoser, "The origin of life cannot be discovered, as in other things in science; it can only be 'reinvented'(*19*)." It is unknown why Mother Nature selects flavin over some other prebiotic flavin mimics, for example, O, 5-hydroxypyrimidines, or some other molecules, as the cofactor in assisting thymine dimer repair. However, it will be interesting to further explore these probable prebiotic molecules and their thymine dimer repair properties, and to investigate one of the contributing factors, excited-state lifetime, behind the observed chemistry.

Toward these goals, 5-hydroxypyrimidine and the ability of some other bases to repair thymine dimer will be discussed in the next chapter. Then I will turn my attention to explore the possibility of recruiting one of the explored flavin mimics, O, by a ribozyme model. After that, I will demonstrate our effort on studying O excited-state lifetime in various contexts.

References

1. Gilbert, W. (1986) Origin of life: The RNA world, *Nature 319*, 618-618.

2. Guerrier-Takada, C., Gardiner, K., Marsh, T., Pace, N., and Altman, S. (1983) The RNA moiety of ribonuclease P is the catalytic subunit of the enzyme, *Cell 35*, 849-857.

3. Kruger, K., Grabowski, P. J., Zaug, A. J., Sands, J., Gottschling, D. E., and Cech, T. R. (1982) Self-splicing RNA: autoexcision and autocyclization of the ribosomal RNA intervening sequence of Tetrahymena, *Cell 31*, 147-157.

4. Unrau, P. J., and Bartel, D. P. (1998) RNA-catalysed nucleotide synthesis, *Nature 395*, 260-263.

5. Illangasekare, M., Sanchez, G., Nickles, T., and Yarus, M. (1995) Aminoacyl-RNA synthesis catalyzed by an RNA, *Science 267*, 643-647.

6. Lohse, P. A., and Szostak, J. W. (1996) Ribozyme-catalysed amino-acid transfer reactions, *Nature 381*, 442-444.

7. Lee, N., Bessho, Y., Wei, K., Szostak, J. W., and Suga, H. (2000) Ribozyme-catalyzed tRNA aminoacylation, *Nat. Struct. Biol. 7*, 28-33.

8. Ekland, E. H., and Bartel, D. P. (1996) RNA-catalysed RNA polymerization using nucleoside triphosphates, *Nature 382*, 373-376.

9. Johnston, W. K., Unrau, P. J., Lawrence, M. S., Glasner, M. E., and Bartel, D. P. (2001) RNA-catalyzed RNA polymerization: accurate and general RNA-templated primer extension, *Science 292*, 1319-1325.

10. Lorsch, J. R., and Szostak, J. W. (1994) In vitro evolution of new ribozymes with polynucleotide kinase activity, *Nature 371*, 31-36.

11. Dai, X., De Mesmaeker, A., and Joyce, G. F. (1995) Cleavage of an amide bond by a ribozyme, *Science 267*, 237-240.

12. Bartel, D. P., and Szostak, J. W. (1993) Isolation of new ribozymes from a large pool of random sequences [see comment], *Science 261*, 1411-1418.

13. Lincoln, T. A., and Joyce, G. F. (2009) Self-sustained replication of an RNA enzyme, *Science 323*, 1229-1232.

14. Zhang, B., and Cech, T. R. (1997) Peptide bond formation by in vitro selected ribozymes, *Nature 390*, 96-100.

15. Nissen, P., Hansen, J., Ban, N., Moore, P. B., and Steitz, T. A. (2000) The structural basis of ribosome activity in peptide bond synthesis, *Science 289*, 920-930.

16. Joyce, G. F. (2002) The antiquity of RNA-based evolution, *Nature 418*, 214-221.

17. Chen, X., Li, N., and Ellington, A. D. (2007) Ribozyme catalysis of metabolism in the RNA world, *Chem. Biodivers. 4*, 633-655.

18. Mills, D. R., Peterson, R. L., and Spiegelman, S. (1967) An extracellular Darwinian experiment with a self-duplicating nucleic acid molecule, *Proc. Natl. Acad. Sci. U.S.A. 58*, 217-224.

19. Eschenmoser, A. (2007) The search for the chemistry of life's origin, *Tetrahedron 63*, 12821-12844.

20. Taylor, J.-S. (1990) DNA, sunlight, and skin cancer, *J. Chem. Educ. 67*, 835.

21. Le May, N., Egly, J. M., and Coin, F. (2010) True lies: the double life of the nucleotide excision repair factors in transcription and DNA repair, *J. Nucleic Acids 2010*.

22. Reardon, J. T., and Sancar, A. (2003) Recognition and repair of the cyclobutane thymine dimer, a major cause of skin cancers, by the human excision nuclease, *Genes Dev. 17*, 2539-2551.

23. Liu, Y., Prasad, R., Beard, W. A., Kedar, P. S., Hou, E. W., Shock, D. D., and Wilson, S. H. (2007) Coordination of steps in single-nucleotide base excision repair mediated by apurinic/apyrimidinic endonuclease 1 and DNA polymerase beta, *J. Biol. Chem. 282*, 13532-13541.

24. Sancar, A. (2003) Structure and function of DNA photolyase and cryptochrome blue-light photoreceptors, *Chem. Rev. 103*, 2203-2237.

25. Holland, H. D. (2002) Volcanic gases, black smokers, and the great oxidation event, *Geochim. Cosmochim. Acta 66*, 3811-3826.

26. Burrows, C. J., and Muller, J. G. (1998) Oxidative Nucleobase Modifications Leading to Strand Scission, *Chem. Rev. 98*, 1109-1152.

27. Begley, T., Kinsland, C., Taylor, S., Tandon, M., Nicewonger, R., Wu, M., Chiu, H.-J., Kelleher, N., Campobasso, N., and Zhang, Y. (1998) Cofactor Biosynthesis: A Mechanistic Perspective, In *Biosynthesis* (Leeper, F., and Vederas, J., Eds.), pp 93-142, Springer Berlin Heidelberg.

28. White, H. B., 3rd. (1976) Coenzymes as fossils of an earlier metabolic state, *J. Mol. Evol. 7*, 101-104.

29. Yarus, M. (2011) Getting past the RNA world: the initial Darwinian ancestor, *Cold Spring Harb. Perspect. Biol. 3*.

30. Smith, S. B., and Bruice, T. C. (1975) Mechanisms of isoalloxazine (flavine) hydrolysis, *J. Am. Chem. Soc. 97*, 2875-2881.

31. Kemal, C., and Bruice, T. C. (1976) Simple synthesis of a 4a-hydroperoxy adduct of a 1,5-dihydroflavine: preliminary studies of a model for bacterial luciferase, *Proc. Natl. Acad. Sci. U.S.A. 73*, 995-999.

32. Massey, V. (1994) Activation of molecular oxygen by flavins and flavoproteins, *J. Biol. Chem. 269*, 22459-22462.

33. Luo, W., Muller, J. G., and Burrows, C. J. (2001) The pH-dependent role of superoxide in riboflavin-catalyzed photooxidation of 8-oxo-7,8-dihydroguanosine, *Org. Lett. 3*, 2801-2804.

34. Luo, W., Muller, J. G., Rachlin, E. M., and Burrows, C. J. (2001) Characterization of hydantoin products from one-electron oxidation of 8-oxo-7,8-dihydroguanosine in a nucleoside model, *Chem. Res. Toxicol. 14*, 927-938.

35. Henderson, P. T., Delaney, J. C., Muller, J. G., Neeley, W. L., Tannenbaum, S. R., Burrows, C. J., and Essigmann, J. M. (2003) The hydantoin lesions formed from oxidation of 7,8-dihydro-8-oxoguanine are potent sources of replication errors in vivo, *Biochemistry 42*, 9257-9262.

36. Ye, Y., Muller, J. G., Luo, W., Mayne, C. L., Shallop, A. J., Jones, R. A., and Burrows, C. J. (2003) Formation of 13C-, 15N-, and 18O-labeled guanidinohydantoin from guanosine oxidation with singlet oxygen. Implications for structure and mechanism, *J. Am. Chem. Soc. 125*, 13926-13927.

37. Misiaszek, R., Uvaydov, Y., Crean, C., Geacintov, N. E., and Shafirovich, V. (2005) Combination reactions of superoxide with 8-Oxo-7,8-dihydroguanine radicals in DNA: kinetics and end products, *J. Biol. Chem. 280*, 6293-6300.

38. Yun, B. H., Lee, Y. A., Kim, S. K., Kuzmin, V., Kolbanovskiy, A., Dedon, P. C., Geacintov, N. E., and Shafirovich, V. (2007) Photosensitized oxidative DNA damage: from hole injection to chemical product formation and strand cleavage, *J. Am. Chem. Soc. 129*, 9321-9332.

39. Munk, B. H., Burrows, C. J., and Schlegel, H. B. (2008) An exploration of mechanisms for the transformation of 8-oxoguanine to guanidinohydantoin and

spiroiminodihydantoin by density functional theory, *J. Am. Chem. Soc. 130*, 5245-5256.

40. Crean, C., Lee, Y. A., Yun, B. H., Geacintov, N. E., and Shafirovich, V. (2008) Oxidation of guanine by carbonate radicals derived from photolysis of carbonatotetramminecobalt(III) complexes and the pH dependence of intrastrand DNA cross-links mediated by guanine radical reactions, *ChemBioChem 9*, 1985-1991.

41. Xu, X., Muller, J. G., Ye, Y., and Burrows, C. J. (2008) DNA-protein cross-links between guanine and lysine depend on the mechanism of oxidation for formation of C5 vs C8 guanosine adducts, *J. Am. Chem. Soc. 130*, 703-709.

42. Johansen, M. E., Muller, J. G., Xu, X., and Burrows, C. J. (2005) Oxidatively induced DNA-protein cross-linking between single-stranded binding protein and oligodeoxynucleotides containing 8-oxo-7,8-dihydro-2'-deoxyguanosine, *Biochemistry 44*, 5660-5671.

43. Hosford, M. E., Muller, J. G., and Burrows, C. J. (2004) Spermine participates in oxidative damage of guanosine and 8-oxoguanosine leading to deoxyribosylurea formation, *J. Am. Chem. Soc. 126*, 9540-9541.

44. Bruice, T. C. (1980) Mechanisms of flavin catalysis, *Acc. Chem. Res. 13*, 256-262.

45. Liang, M. C., Hartman, H., Kopp, R. E., Kirschvink, J. L., and Yung, Y. L. (2006) Production of hydrogen peroxide in the atmosphere of a Snowball Earth and the origin of oxygenic photosynthesis, *Proc. Natl. Acad. Sci. U.S.A. 103*, 18896-18899.

46. Nguyen, K. V., and Burrows, C. J. (2011) A prebiotic role for 8-oxoguanosine as a flavin mimic in pyrimidine dimer photorepair, *J. Am. Chem. Soc. 133*, 14586-14589.

47. Nguyen, K. V., and Burrows, C. J. (2012) Photorepair of cyclobutane pyrimidine dimers by 8-oxopurine nucleosides, *J. Phys. Org. Chem. 25*, 574-577.

48. Liu, Z., Tan, C., Guo, X., Kao, Y. T., Li, J., Wang, L., Sancar, A., and Zhong, D. (2011) Dynamics and mechanism of cyclobutane pyrimidine dimer repair by DNA photolyase, *Proc. Natl. Acad. Sci. U.S.A. 108*, 14831-14836.

49. Kim, S. T., Hartman, R. F., and Rose, S. D. (1990) Solvent dependence of pyrimidine dimer splitting in a covalently linked dimer-indole system, *Photochem. Photobiol. 52*, 789-794.

50. Carell, T., and Epple, R. (1998) Repair of UV Light Induced DNA Lesions: A Comparative Study with Model Compounds, *Eur. J. Org. Chem. 1998*, 1245-1258.

51. Song, Q.-H., Tang, W.-J., Hei, X.-M., Wang, H.-B., Guo, Q.-X., and Yu, S.-Q. (2005) Efficient Photosensitized Splitting of Thymine Dimer by a Covalently Linked Tryptophan in Solvents of High Polarity, *Eur. J. Org. Chem. 2005*, 1097-1106.

52. Epple, R., Wallenborn, E.-U., and Carell, T. (1997) Investigation of Flavin-Containing DNA-Repair Model Compounds, *J. Am. Chem. Soc. 119*, 7440-7451.

53. Song, Q.-H., Tang, W.-J., Ji, X.-B., Wang, H.-B., and Guo, Q.-X. (2007) Do Photolyases Need To Provide Considerable Activation Energy for the Splitting of Cyclobutane Pyrimidine Dimer Radical Anions?, *Chem. Eur. J. 13*, 7762-7770.

54. Kao, Y. T., Song, Q. H., Saxena, C., Wang, L., and Zhong, D. (2012) Dynamics and mechanism of DNA repair in a biomimetic system: flavin-thymine dimer adduct, *J. Am. Chem. Soc. 134*, 1501-1503.

55. Pecourt, J. M., Peon, J., and Kohler, B. (2001) DNA excited-state dynamics: ultrafast internal conversion and vibrational cooling in a series of nucleosides, *J. Am. Chem. Soc. 123*, 10370-10378.

56. Rios, A. C., and Tor, Y. (2013) On the Origin of the Canonical Nucleobases: An Assessment of Selection Pressures across Chemical and Early Biological Evolution, *Isr. J. Chem. 53*, 469-483.

57. Takaya, T., Su, C., de La Harpe, K., Crespo-Hernandez, C. E., and Kohler, B. (2008) UV excitation of single DNA and RNA strands produces high yields of exciplex states between two stacked bases, *Proc. Natl. Acad. Sci. U.S.A. 105*, 10285-10290.

58. Bucher, D. B., Schlueter, A., Carell, T., and Zinth, W. (2014) Watson-crick base pairing controls excited-state decay in natural DNA, *Angew. Chem. Int. Ed. 53*, 11366-11369.

59. Kumar, A., and Sevilla, M. D. (2013) Excited state proton-coupled electron transfer in 8-oxoG-C and 8-oxoG-A base pairs: a time dependent density functional theory (TD-DFT) study, *Photochem. Photobiol. Sci. 12*, 1328-1340.

60. Rios, A. C., and Tor, Y. (2012) Refining the genetic alphabet: a late-period selection pressure?, *Astrobiology 12*, 884-891.

61. Yanagawa, H., Ogawa, Y., and Ueno, M. (1992) Redox ribonucleosides. Isolation and characterization of 5-hydroxyuridine, 8-hydroxyguanosine, and 8-hydroxyadenosine from Torula yeast RNA, *J. Biol. Chem. 267*, 13320-13326.

62.	Riviere, J., Bergeron, F., Tremblay, S., Gasparutto, D., Cadet, J., and Wagner, J. R. (2004) Oxidation of 5-hydroxy-2'-deoxyuridine into isodialuric acid, dialuric acid, and hydantoin products, *J. Am. Chem. Soc. 126*, 6548-6549.

63.	Nachtigallova, D., Lischka, H., Szymczak, J. J., Barbatti, M., Hobza, P., Gengeliczki, Z., Pino, G., Callahan, M. P., and de Vries, M. S. (2010) The effect of C5 substitution on the photochemistry of uracil, *Phys. Chem. Chem. Phys. 12*, 4924-4933.

64.	Yanagawa, H., Ogawa, Y., Ueno, M., Sasaki, K., and Sato, T. (1990) Search for novel RNA catalysts. An RNA component with oxidoreductase activity, *Nucleic Acids Symp. Ser.*, 61-62.

65.	Havelund, J. F., Giessing, A. M., Hansen, T., Rasmussen, A., Scott, L. G., and Kirpekar, F. (2011) Identification of 5-hydroxycytidine at position 2501 concludes characterization of modified nucleotides in E. coli 23S rRNA, *J. Mol. Biol. 411*, 529-536.

66.	Banyasz, A., Karpati, S., Mercier, Y., Reguero, M., Gustavsson, T., Markovitsi, D., and Improta, R. (2010) The peculiar spectral properties of amino-substituted uracils: a combined theoretical and experimental study, *J. Phys. Chem. B 114*, 12708-12719.

67.	Baik, M.-H., Silverman, J. S., Yang, I. V., Ropp, P. A., Szalai, V. A., Yang, W., and Thorp, H. H. (2001) Using Density Functional Theory To Design DNA Base Analogues with Low Oxidation Potentials, *J. Phys. Chem. B 105*, 6437-6444.

68.	Sieradzan, I., Marchaj, M., Anusiewicz, I., Skurski, P., and Simons, J. (2014) Prediction of thymine dimer repair by electron transfer from photoexcited 8-aminoguanine or its deprotonated anion, *J. Phys. Chem. A 118*, 7194-7200.

69.	Gengeliczki, Z., Callahan, M. P., Svadlenak, N., Pongor, C. I., Sztaray, B., Meerts, L., Nachtigallova, D., Hobza, P., Barbatti, M., Lischka, H., and de Vries, M. S. (2010) Effect of substituents on the excited-state dynamics of the modified DNA bases 2,4-diaminopyrimidine and 2,6-diaminopurine, *Phys. Chem. Chem. Phys. 12*, 5375-5388.

70.	Kawai, K., Kodera, H., and Majima, T. (2010) Long-range charge transfer through DNA by replacing adenine with diaminopurine, *J. Am. Chem. Soc. 132*, 627-630.

71.	Tsukiji, S., Pattnaik, S. B., and Suga, H. (2003) An alcohol dehydrogenase ribozyme, *Nat. Struct. Biol. 10*, 713-717.

72. Tsukiji, S., Pattnaik, S. B., and Suga, H. (2004) Reduction of an aldehyde by a NADH/Zn2+ -dependent redox active ribozyme, *J. Am. Chem. Soc. 126*, 5044-5045.

CHAPTER 2

OXIDIZED PYRIMIDINES IN CYCLOBUTANE PYRIMIDINE

DIMER REPAIR

Introduction

The RNA world hypothesis suggests that ancient life originated from RNA oligomers

due to their propensity to both store genetic information and catalyze reactions (*1*). Critical

to this hypothesis is the findings that RNA could catalyze chemical transformations nearly

as diverse as protein enzymes do (*2, 3, 4, 5, 6, 7, 8*). A prominent example of extant RNA

enzymes, or ribozymes, is the ribosome (*9*). Studies have shown life may have originated

as early as the Archaean eon (*10*). However, due to the lack of ozone layer protection and

genome repair machinery on primordial Earth, the hypothesized ribonucleic acid bases

would have been undergoing constant assault by radiation and species generated from

possible oxidation processes such as Fenton chemistry (*11, 12*). In the contemporary world,

these oxidative damages could be mitigated by various repair enzymes. Redox enzymes

are one of the major classes of enzymes that are used to repair these damages. However,

these enzymes usually have to recruit nucleotide cofactors (NADH, $FADH_2$, pterins, or

metal complexes) to facilitate oxidation and reduction processes. This is because neither

the four RNA bases nor the canonical amino acids are very redox active. Interestingly,

many of these cofactors contain an RNA component, adenosine. Thus, it was hypothesized

that they likely evolved from the four ribonucleotide bases, A, C, G, and U, or coevolved as separate nucleotide components (*13*). A recent hypothesis has placed these dinucleotide cofactors at a critical juncture called the Initial Darwinian Ancestor (IDA) (*14*). Considering the complex structure of extant redox cofactors, it is hard to imagine how these cofactors could have been formed on the primordial earth. Instead, we are interested in searching among known RNA bases and their derivatives for possible substitutes for extant cofactors (*13*).

We hypothesize that some oxidatively modified ribonucleotide bases could have predated the sophisticated cofactor molecules as primordial cofactors. Among them, 5-hydroxydeoxycytidine (5-HC) is a common pyrimidine lesion encountered in genomic DNA due to the ubiquitous presence of reactive oxygen species (ROS) (*15*). This is equally true for the RNA version of 5-HC. It has been detected in yeast RNA and *E. coli* 23S rRNA (*16, 17*) even though its function is currently unknown. Remarkably, upon incorporation of a hydroxyl group at 5-position of C, the redox potential of the resulting modified base is decreased by almost 1 V (Scheme 2.1). It has been shown that two-electron oxidation of 5-HC could generate an NAD^+ like species which could be reduced by NADH (*18*). 8-Oxo-7,8-dihydro-2'-deoxyguanosine (O) was recently reported to mimic a flavin cofactor in catalyzing photo-initiated excess electron transfer (EET) repairing nearby pyrimidine dimer (*13, 19, 20*). The underlying mechanism is proposed to be similar to photolyase catalysis process, i.e., photo-excited O could donate one electron to the thymine dimer, followed by back electron transfer (ET) from repaired thymine dimer regenerating O. This hypothesis is based on the fact that O has a lower redox potential compared to G. Considering that the redox potential of 5-HC (0.78 V) is similar to that of O (0.74 V) (*18*),

Scheme 2.1 A common oxidatively modified product of cytidine (5-HC) exhibits novel redox properties.

we hypothesized that 5-HC can also mimic the flavin cofactor in mediating photo-induced electron transfer repair of a thymine dimer.

The purines and their derivatives affecting thymine dimer repair and/or formation have been the subject of several recent investigations (*21, 22, 23, 24, 25, 26*). Even though it is observed that a flanking pyrimidine base, especially at the 5' position of a thymine dimer, could enhance the formation of thymine dimer upon UV irradiation (*27*), the repair of thymine dimer by a flanking pyrimidine base, as far as we know, has not been thoroughly studied.

To systematically investigate the possibility of 5-HC-catalyzed photo-initiated EET repair of thymine dimer, we incorporated 5-HC (for ease of handling and preparation, we did not use the RNA version) into the previously used system by phosphoramidite chemistry. In this chapter, we first discuss how the incorporation of 5-HC into a DNA duplex affects the stability of thymine dimer containing duplex DNA. Next, we demonstrate thymine dimer repair in dsDNA and ssDNA by photo irradiation of 5-HC. Finally, we report thymine dimer can also be repaired in dsDNA by photo-irradiated 5-hydroxydeoxyuridine (5-HU), 2-amino dA (or 2, 6-diaminopurine, D), and 8-amino dG (R).

Results and discussions

Design, synthesis, and stability of 5-HC containing dsDNA. The redox property of 5-HC (along with 5-hydroxyuridine, 8-oxo-7,8-dihydroguanine, and 8-oxo-7,8-dihydroadenosine) has been well documented by Yanagawa et al. (*18*). Our hypothesis is based on the fact that the one electron reduction potential for 5-HC is low enough to

produce the Gibbs free energy for the repair of a thymine dimer reaction via ET to be negative, thus this reaction would be thermodynamically feasible (*28*). 5-HC (designated as "X" in sequences in Chart 2.1) was incorporated into thymine dimer containing dsDNA using standard phosphoramidite chemistry. To simplify later analysis, the two complementary strands were designed to have different lengths that could be easily separated on a denaturing HPLC column. We incorporated X and thymine dimer in various locations as shown in Chart 2.1. Thymine dimer is incorporated into the top, short strand; 5-HC is installed on either top, short or bottom, long strand. These sequences will allow us to study strand, directional, distance, and base pair effects on excess electron transfer repair of the thymine dimer.

In order to investigate the impact of thymine dimer and 5-HC incorporation on dsDNA stability as well as the base recognition preference of 5-HC in a dsDNA context, we collected data for the melting curve of these modified duplexes at 260 nm. The corresponding T_m data were obtained from the maxima of the first derivatives of the melting curves and summarized in Table 2.1. The T_m data derived from the above experiments reveal that the preferred pairing base of 5-HC is G (T_m=53.0-55.8 °C) over A (T_m=43.9-44.6 °C). A mismatched base pair with A significantly destabilizes the duplex (*29*). The absence of a pairing base further reduces the stability of the duplex more for **8F** (T_m=39.7 °C) than for **7F** (T_m=42.3 °C), suggesting less base stacking at this position caused by the adjacent thymine dimer, consistent with previous reports (*30, 31*). dsDNAs with 5-HC on the bottom strand (**1G** and **2G**) are more stable than with 5-HC on the top strand (**7G** and **8G**). This is probably due to better base stacking with alternating pyrimidine and purine bases in **1G** and **2G** than with three consecutive pyrimidine bases

1G	CAC AGC GT=T ACA GTA CAC TCT GTG TCG XA A TGT CAT GTG T		**8G**	CAC AGC AT=T XCA GTA CAC TCT GTG TCG TA A GGT CAT GTG T
2G	CAC AGC AT=T GCA GTA CAC TCT GTG TCG TA A XGT CAT GTG T		**7A**	CAC AGC XT=T ACA GTA CAC TCT GTG TCG AA A TGT CAT GTG T
1A	CAC AGC AT=T ACA GTA CAC TCT GTG TCG XA A TGT CAT GTG T		**8A**	CAC AGC AT=T XCA GTA CAC TCT GTG TCG TA A AGT CAT GTG T
2A	CAC AGC AT=T ACA GTA CAC TCT GTG TCG TA A XGT CAT GTG T		**7F**	CAC AGC XT=T ACA GTA CAC TCT GTG TCG FA A TGT CAT GTG T
3	CAC AGC AT=T ACA GTA CAC TCT GTG TCG TX A TGT CAT GTG T		**8F**	CAC AGC AT=T XCA GTA CAC TCT GTG TCG TA A FGT CAT GTG T
4	CAC AGC AT=T ACA GTA CAC TCT GTG TCG TA X TGT CAT GTG T		**9G**	ACA GCX AT=T ACA GTA CAC TCT TGT CGG TA A TGT CAT GTG T
5	CAC AGG AT=T ACA GTA CAC TCT GTG TCX TA A TGT CAT GTG T		**10G**	CAC AGC AT=T AXC AGT ACA TCT GTG TCG TA A TGG TCA TGT T
6	CAC AGC AT=T AGA GTA CAC TCT GTG TCG TA A TXT CAT GTG T		**9F**	ACA GCX AT=T ACA GTA CAC TCT TGT CGF TA A TGT CAT GTG T
7G	CAC AGC XT=T ACA GTA CAC TCT GTG TCG GA A TGT CAT GTG T		**10F**	CAC AGC AT=T AXC AGT ACA TCT GTG TCG TA A TFG TCA TGT T
7S	CAC AGC XT=T ACA GTA CAC		**9S**	ACA GCX AT=T ACA GTA CAC
8S	CAC AGC AT=T XCA GTA CAC		**10S**	CAC AGC AT=T AXC AGT ACA

Chart 2.1 Sequences of 5-HC and thymine dimer containing dsDNA and ssDNA where X stands for 5-hydroxydeoxypyrimidine, and F stands for tetrahydrofuran abasic site.

Table 2.1 T_m data (°C, 260 nm) of dsDNA. Duplex concentration: 2 μM in 20 mM sodium borate, 100 mM NaCl, pH 8.5 buffer

	T_m		T_m
1G	54.4±0.4	**8F**	39.7±0.4
2G	55.8±0.6	**9G**	53.0±0.4
1A	44.5±0.3	**10G**	52.2±0.4[a]
3	45.7±1.6	**9F**	38.5±0.1
4	42.9±0.1	**10F**	38.6±0.7
7G	53.0±0.3, 42.4±0.4	**1G**[b]	57.5±0.2[a]
8G	53.8±0.8[a]	**1G**[c]	58.5±0.3
7A	43.9±0.2	**7G**[d]	53.6±0.6
8A	44.6±0.1	**1A**[e]	52.1±0.2
7F	42.3±0.3	**1G**[e]	48.4±0.1

[a]There is also a low melting transition for this sequence; however, the melting temperature could not be determined (see Supporting Information). [b]Two thymine monomers instead of thymine dimer. [c]X=C and two thymine monomers instead of thymine dimer. [d]X=C. [e]X=5-HU.

in **7G** and **8G**. Direct base pairing with a T of the thymine dimer also destabilizes the duplex, with 5-HC pairing with the 3'-T less stable than with the 5'-T. It was already known that the formation of a thymine dimer causes conformational distortion, primarily on the 5'-side (*30, 31*). Mismatch base pairing with the 3'-T of the thymine dimer could further destabilize the duplex (*32*). Even though 5-HC could form a Watson-Crick base pair with G, the base pairing pattern could be perturbed due to the presence of the 5-hydroxy group. A biphasic melting curve was previously observed in 5-HC containing dsRNA (*33*). Hydrogen bonding between the 5-hydroxyl group and the 5'-phosphate group has been proposed as the cause of this biphasic behavior. We also observed a biphasic melting pattern in sequence **7G** (Figure 2.1) although it was less evident than in dsRNA. This biphasic pattern was confirmed to be caused by the presence of 5-HC as replacing it with C (Figure 2.1) re-established the classical monophasic denaturing pattern. This biphasic pattern could also be observed in sequence **1G** with repaired thymine dimer. Similarly, replacing 5-HC with C could also abrogate the biphasic pattern. However, for other 5-HC containing sequences, the biphasic pattern is not apparent or undetectable, suggesting a synergic effect of 5-HC:G base pair formation and the presence of a thymine dimer.

The base pairing preference of 5-hydroxy-2'-deoxyuridine (5-HU) was also studied in thymine dimer containing dsDNA. Even though experimental (*34*) and theoretical (*35, 36*) studies showed G as the preferred pairing base in dsDNA, we find that having A as the pairing base in thymine dimer containing dsDNA is more stable than that of having G. This is consistent with the result from 5-HU containing DNA-RNA heteroduplex which shows A is the preferred pairing base (*37*).

pH effect on photo-induced thymine dimer repair. To avoid self-repair mediated
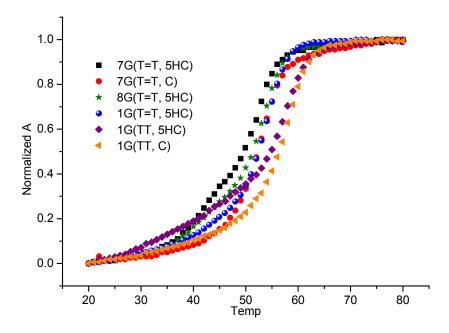
Figure 2.1 Melting curve of some typical duplexes. Conditions: 2 μM duplex in 20 mM sodium borate, 100 mM NaCl, pH 8.5 buffer.

by either direct excitation of thymine dimer with 254 nm light or excitation of other bases, especially G(*22*), followed by electron transfer to the thymine dimer, we decide to use light above 300 nm at which both thymine dimers and canonical bases are virtually transparent. This will significantly reduce the background self-repair. The maximum absorbance of cytosine is red-shifted to 318 nm upon incorporation of the 5-hydroxy group. Significant absorbance above 300 nm allows us to direct light at this particular base. The proton on the 5-hydroxyl group is quite acidic with pK_a value determined to be 7.4 for the nucleoside (*38*). This readily dissociable proton is responsible for the pH-dependent UV absorbance (*16, 39*).

Deprotonation of the 5-hydroxyl group appears to red-shift the maximum absorbance and render a better electron-donating group. Thus, a faster repair process is expected at higher pH. Sequence **1G** was annealed in pH 7.0, 7.5, 8.0, 8.5, 9.0, and 9.5 buffers. The resulting duplexes were irradiated in polystyrene cuvettes using a 40 W UVB light source (λ_{max}=313 nm). The duplexes were then subjected to denaturing HPLC analysis (Figure 2.2A). The yield of repaired T=T strands could be calculated using the peak areas normalized against extinction coefficients of each strand. The calculated yields were fitted to a first-order kinetic model (Figure 2.2B). The repair rates were then plotted for each pH condition (Figure 2.2C). From the graph, an apparent pH-dependent pattern could be observed. Increasing the buffer pH from 7.0 to 7.5 has little effect on the repair rate. However, further increasing the pH significantly increases the repair rate. The repair rate reaches maxima around pH 9.0. It decreases at even higher pH, likely caused by DNA instability. This is consistent with the observation that UV absorbance of 5-HC is pH-dependent (*39*). Based on a UV spectrophotometric pH titration study, its absorbance at
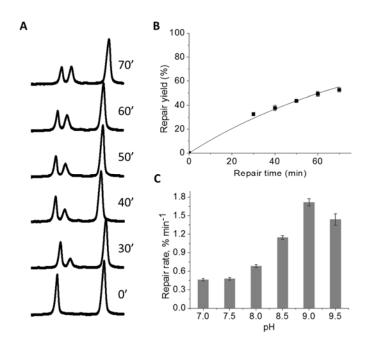
Figure 2.2 Thymine dimer repair analysis. A) Typical denaturing HPLC traces of the irradiated duplex. Thymine dimer strand elutes first, followed by repaired thymine dimer strand. The bottom long strand elutes last. B) Plot of calculated repair yield vs. repair time. The data are fitted according to first-order kinetics. A repair rate could be generated by fitting the data. C) Repair rate of sequence **1G** at different pH values.

318 nm increases sharply from pH 6 to pH 8, with a transition around 7.4, corresponding to the pK_a of 5-hydroxyl group of 5-HC. However, these numbers should be calibrated by 1.1 units by considering the presence of a 5'-phosphate group which is thought to increase the pK_a of 5-hydroxyl group from 7.4 to 8.5 (*38*). Due to DNA stability and deamination issues at higher pH and also to make a comparison with the previous experiment (**1A** in ref. (*19*)), we choose to investigate this further using a pH 8.5 buffer.

Directional effects on photo-induced thymine dimer repair. After establishing that a 5-HC placed on the 5- side of the thymine dimer (sequence **1G**) could repair the thymine dimer, we tested whether 5-HC on the 3'-side of T=T (sequence **2G**) could also repair the dimer. Previously, it has been shown that a flanking O on 5'-side of T=T has a higher repair rate than O on 3'-side of T=T (*19*). Similarly, we observed the repair from 3'-side is 2.7-fold less efficient than the repair from 5'-side (Figure 2.3), demonstrating the same directional preference as in the O experiment. This is explained based on the findings from NMR and crystal structure studies that base stacking on the 3'-side of dimer is disturbed more than that on 5'-side of dimer (*30, 31*). Base stacking has been shown to favor a charge transfer state (*40, 41*). Thus, a higher repair yield by 5-HC from the 5' side may originate from better base stacking with T=T. It has also been shown that the mode of base stacking could lead to electron transfer directional preference of 5' to 3' along DNA duplex which is opposite to a typical 3'-5' preference (*42*).

Due to asymmetric orbital overlap of adjacent bases (*43*), excess electron transfer from the 3' to 5' direction is preferred (*44, 45*). We could also observe this electron transfer directional preference as shown in sequence **10G** which is 2.6-fold faster than in sequence **9G**. These two sequences have one intervening base pair in between 5-HC and the dimer.
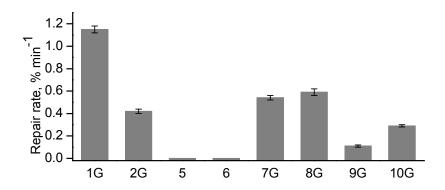
Figure 2.3 Directional and strand effects on the rate of photo-induced (>300 nm) EET repair of thymine dimer in 5-HC containing dsDNA. Conditions: annealed 5 μM top strand and 1.3 equivalent bottom strand in 20 mM sodium borate, 100 mM NaCl, pH 8.5.

The base stacking disturbance by thymine dimer in a more remote position from 5-HC is expected to be minimal, thus asymmetric orbital overlap rather than base stacking may be the predominant factor determining electron transfer along DNA even though a low melting transition could be observed in sequence **10G**.

Strand effects on photo-induced thymine dimer repair. In B-DNA, interstrand base-base orbital coupling is minimal compare to intrastrand coupling. Thus, an electron transfer process needs to overcome a higher barrier to transfer through strands compared to along strands. It has been observed that intrastrand electron transfer is faster than interstrand electron transfer. Thus, we would expect a higher repair rate for sequence **7G** than for sequence **1G**. On the contrary, we observed a 2.1-fold decrease of repair efficiency for sequence **7G** (Figure 2.3). The only difference between these two sequences is that 5-HC is on the top strand, flanking the thymine dimer, in sequence **7G** while it is on the bottom strand in sequence **1G**. One explanation we can envision is that in sequence **7G**, there are three consecutive pyrimidine (CXT) bases which has been proposed before to have less orbital coupling among bases, thus affecting the exciplex formation between 5-HC and 5'-T of dimer. Base stacking may play a role in this case as a thermal study shows that sequence **7G** (T_m=53.0 °C) is less stable than sequence **1G** (T_m=54.4 °C). This stability issue can also be observed in sequence **8G** (T_m=53.8 °C) and **2G** (T_m=55.8 °C). Thus, better base stacking may account for the observed repair rate difference. However, we could not rule out other possibilities, especially an extrahelical position of 5-HC due to its poor H-bonding with dG proposed in ref (*46*). The poor H-bonding behavior was thought to be due to hydroxyl substitution on C5 of dC. An NMR study showed that there is likely a hydrogen bond between the 5-hydroxy group and the 5'-phosphate of 5-HC monophosphate (*38*).

However, it is not clear if this hydrogen bond interaction exists in the duplex DNA structure. A thermal melting study showed that a 5-HC containing dsRNA could adopt, besides a standard Watson-Crick structure, a low stability conformation (*33*). Imperfect base pair formation with G induced by hydrogen bonding between the 5-hydroxy group and a 5'-phosphate group is proposed as the cause of the low-stability conformation. We could also observe a low melting conformation in 5-HC containing dsDNA. A thermal melting study of 5-HC and thymine dimer containing dsDNA shows that this low stability conformation (T_m=42.4 °C) behaves like a mismatch structure as in sequence **7A** (T_m=43.9 °C). Surprisingly, this behavior is only apparent in sequence **7G** but not in sequence **1G**. This low-stability conformation may exacerbate the already poor base stacking between 5-HC and 5'-T of the dimer. The less stable conformation also exists in sequence **8G** though the melting temperature could not be successfully determined (Figure 2.1). We hypothesize that this could also be the cause of low repair rate for sequence **8G** compared to sequence **2G**. Despite this observed repair rate discrepancy, the fact that intrastrand electron transfer is inherently more efficient than interstrand electron transfer is corroborated when there is one intervening base pair between 5-HC and thymine dimer (see **5** vs. **9G** and **6** vs. **10G** in Figure 2.3).

Base-pair and distance effects on photo-induced thymine dimer repair. Better base stacking is expected in an ideal Watson-Crick base pair. A mismatch or absence of a pairing base can lead to a less stable duplex structure as is evidenced in Table 2.1 (**1G** vs. **1A**, **7G** vs. **7A** vs. **7F**, **8G** vs. **8A** vs. **8F**, **9G** vs. **9F**, **10G** vs. **10F**). In all cases, switching from a Watson-Crick base pair to a mismatched base pair destabilizes the duplex structure (*29*). Absence of a pairing base (i.e. opposite an abasic site analog F) further exacerbates the

destabilization. The sequences **1G**, **7G**, and **8G** may be especially sensitive to base pairing due to the proximity of the modified base to the thymine dimer. The base pairs may be essential to hold the duplex together and have better base stacking which is important for an efficient repair rate (**1G** vs. **1A**, **7G** vs. **7A** vs. **7F**, **8G** vs. **8A** vs. **8F** in Figure 2.4). However, sequences **9G** and **10G** are insensitive to the base pair effect or the lack of pairing base does not affect base stacking with neighboring bases (**9G** vs. **9F**, **10G** vs. **10F** in Figure 2.4), presumably due to diminished structural perturbation by the thymine dimer at these positions. In sequences **3** and **4**, 5-HC directly pairs with a T of the thymine dimer. Even though the 3'-T mismatched base pair in sequence **4** (T_m=42.9 °C) is thermodynamically less stable than the 5'-T mismatched base pair in sequence **3** (T_m=45.7 °C), its repair rate is 1.6-fold faster than that of sequence **3** (Figure 2.4). However, it is still less efficient than sequence **1G**. We do not have a good explanation for this phenomenon at this time. It may reflect the inherently efficient direct electron transfer to, and back electron transfer from, the 3'-T, or efficient charge recombination between the 5' positioned 5-HC$^{+\bullet}$ and T=T$^{-\bullet}$.

Repair of a thymine dimer by 5-HC located one base further away from the dimer is usually slower. In the case of intrastand repair, a 2- and 5-fold decrease in repair rate is observed in sequences **8G** and **10G** and sequences **7G** and **9G**, respectively (Figure 2.4). For interstrand repair, we did not observe any thymine dimer repair after 2 h irradiation in sequences **5** and **6** (Table 2.2 and Figure 2.3) in contrast to efficient repair with short distance as in sequences **1G** and **2G**.

Photo-induced thymine dimer repair in single-strand DNA. 5-HC can repair a thymine dimer not only in the dsDNA context but also in a ssDNA context. The repair
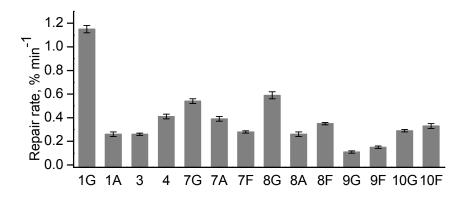
Figure 2.4 Base-pair and distance effects on the rate of photo-induced (>300 nm) EET repair of thymine dimer in 5-HC containing dsDNA. Conditions: annealed 5 μM top strand and 1.3 equivalent bottom strand in 20 mM sodium borate, 100 mM NaCl, pH 8.5.

Table 2.2 Rate of photo-induced (>300 nm) EET repair of thymine dimer in 5-hydroxypyrimidine containing dsDNA. Condition: annealed 5 μM top strand and 1.3 equiv. bottom strand in 20 mM sodium borate, 100 mM NaCl, pH 8.5 for 2 h.

Sequence	Repair rate
5	n.d.[a, b, c]
6	n.d.[a, b, c]
1G[c]	22±2%
1A[c]	34±2%
2A[c]	14±1%
[a]No repair is detected up to 2 h irradiation. [b]X=5-HC. [c]X=5-HU.	

process is proposed to follow excess electron transfer (EET) mechanism as hole transfer does not operate in ssDNA at all (*47*). Thymine dimer repair and formation in ssDNA using 240 nm or 280 nm light have been reported, featuring thymine flanked by purine bases (*19, 24, 25*). A 5'-purine has been shown to repair dimer faster or inhibit the formation of the dimer more than a 3'-purine. This 5'-purine preference is consistent with that observed in dsDNA or hairpin context. A preference in ssDNA has been previously attributed to a quenching effect by the flanking purine base on the excited state of the dimer. However, for thymine dimer containing ssDNA flanked by modified pyrimidine bases, we observed an opposite trend in the photorepair process (Figure 2.5). In our case, repair of a thymine dimer by a 3'-5-HC in sequence **8S** is 2.5-fold faster than that in sequence **7S**. An EET mechanism is thought to operate in ssDNA. Thymine dimer absorbance at >300 nm is negligible. Thus, direct photoreversion is less likely under these experimental conditions. Even though the structure in ssDNA is dynamic, base stacking has been proposed as the contributing factor for the formation of a long-lived excited state in ssDNA (*41, 48, 49, 50, 51*). Therefore, asymmetric orbital overlap seems to be the plausible explanation for the observed directional effect (*43*). However, we cannot exclude the possibility of better base stacking as the cause of a better repair yield when 5-HC is on the 3' side of the thymine dimer. Excess electron transfer along the DNA strand is well known to be either shallow (*45, 52, 53*) or deeply (*19*) distance dependent. Our experiment shows thymine dimer repair by 5-HC from one base away (**9S** and **10S**) is less efficient than by a flanking 5-HC.

Photo-induced thymine dimer repair in 5-HU containing dsDNA. Deamination of 5,6-dihydroxy-5,6-dihydrocytosine (cytosine glycol) and subsequent dehydration could generate another redox-active modified nucleobase, 5-HU. Its one-electron oxidation pot-
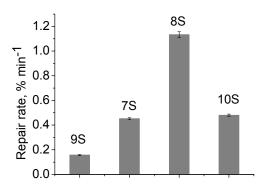
Figure 2.5 Rate of photo-induced (>300 nm) EET repair of thymine dimer in 5-HC containing ssDNA. Conditions: 5 μM ssDNA in 20 mM sodium borate, 100 mM NaCl, pH 8.5.

ential is reported to be similar to 5-HC (*18*). We also incorporated this modified base into dsDNA. The repair of thymine dimer in duplex DNA with a 5'-side flanking 5-HU pairing with A is more efficient than that pairing with G (Table 2.2). It has been reported that 5-HU can form a more stable base pair with G than with A in dsDNA (*34*). However, we found the duplex with a 5-HU:A base pair is more stable than that with a 5-HU:G base pair (ΔT_m=3.7 °C, Table 2.1). This may account for the higher repair rate observed for the duplex with a 5-HU:A base pair. Switching 5-HU:A to the 3'-side of the thymine dimer results in reduced repair yield (Table 2.2). This directional effect could also be explained on the basis of the findings that base stacking on the 3' side is disturbed in the thymine dimer containing duplex. Attempts to repair the thymine dimer from both sides in the duplex with one base pair intervening failed (sequences **5** and **6** in Table 2.2). We did not observe any repair after 2 h irradiation. Overall photo-induced ET repair of a thymine dimer by 5-HU is less efficient than by the cytosine analog. While the oxidation potentials of these modified bases may partially account for the repair differences, base stacking may be responsible for the difference. The G:C base pair has a better base stacking propensity than the A:T base pair (*21*). Another possibility is related to the electron transfer rate between 5-HU and a thymine dimer. A short excited-state lifetime and fast back ET may also contribute to the observed results. A detailed photodynamic study on this needs to done to verify this hypothesis.

Photo-induced thymine dimer repair in 2-amino dA (D) containing dsDNA. The detection of a terrestrially rare nucleobase analog D in a meteorite sample (*54*), which is also accessible via ammonium cyanide chemistry, a purported ingredient in the "prebiotic soup", lends the possibility that this small molecule may also have existed on primordial

Earth. Even though present-day biology rarely uses this molecule anymore, we can speculate about its role in earlier times from known facts: 1) it has a red-shifted UV spectra (λ_{max}=280 nm and absorption tail above 300 nm at pH 7) compared to canonical bases (*55*); 2) its lower oxidation potential (1.2 V vs. NHE) compared to G (1.31 V vs. NHE) (*56*); and 3) long gas phase excited state lifetime, 6.3 ns (*57*). To test our hypothesis, we incorporated this base into a duplex using standard phosphoramidite chemistry, and compared its thymine dimer repair ability to other modified bases. Overall it is less efficient in repairing thymine dimer (Table 2.3). A relatively high redox potential may account for its overall low repair ability. We did not observe any repair difference when D is directly pairing with T. This may be due to stable base pair formation between D and T of thymine dimer. Thus, it may wipe out any inherent repair difference observed in the previous section.

Photo-induced thymine dimer repair in 8-amino dG (R) containing dsDNA. Though the exact redox potential of R is unknown, a few literature reports provide clues that it has an even lower redox potential than O (*58, 59*). A theoretical study has predicted that it has an even better thymine dimer repair efficiency (*60*). The UV spectrum of R is similar to that of O at various pH values (*61*), which allows selective excitation of R. Thus, its thymine dimer repair ability was investigated by putting R directly opposite thymine, likely involving wobble base pairing. After 75 min irradiation, about the same amount of thymine dimer is repaired as in an analogous O experiment. A wobble base pair involving R and the 3' T may be more stable than with the 5' T, and this may account for its higher repair yield. However, when the R:A base pair was placed flanking T=T on either side, the repair yields were much smaller. This may be due to inadequate base pair stability between R and A (*62*) which can destabilize its base stacking with T=T.

Table 2.3 Comparison of thymine dimer repair by various modified bases. Reaction condition: 5 µM DNA in 20 mM NaPi, 100 mM NaCl, pH 7 buffer at rt, 75 min unless otherwise specified.

Entry	Sequence	Irradiation time (min)	Yield (%) 8-aminoG (2-aminoA)
1	AT=TA XA AT	75	13.7±1.1 (12.8±1.8)
2	AT=TA TX AT	75	17.8±1.6 (9.4±0.7)
3	AT=TA TA XT	75	87.0±2.0 (8.1±0.7)
4	AT=TA TA AX	75	26.0±1.3 (12.5±0.9)
5	AT=TA TO AT	75	20[a]
6	AT=TA TA OT	75	82[a]
7	AT=TA T^{5OH}CAT	70	17.1±1.7[b, c]
8	AT=TA TA$^{5\text{-}OH}$CT	70	27.0±1.5[b, c]

a K. V. Nguyen, Ph.D. dissertation, University of Utah, 2012, Chap 3; b Appendix; c In 20 mM sodium borate, 100 mM NaCl, pH 8.5 buffer

Conclusions

In this chapter, we report a role for 5-hydroxypyrimidine bases repairing a nearby thymine dimer upon photo irradiation in dsDNA and ssDNA. The low oxidation potential, oxidatively modified pyrimidine bases are incorporated in thymine dimer containing dsDNA and ssDNA. Depending upon the location of 5-HC in dsDNA, it could induce a biphasic melting process of dsDNA contexts. This phenomenon is shown to be produced by the presence of the 5-hydroxyl group on C. However, the biphasic transition process is not observed in all 5-HC containing dsDNA nor found in 5-HU containing dsDNA. Therefore, it is likely that the biphasic transition is closely related to the local microstructure generated by the thymine dimer and unique features endowed by the 5-HC base.

The propensity of photo-induced excess electron transfer from 5-HC to thymine dimer was studied in the context of dsDNA and ssDNA. We find the repair efficiency is closely related to the buffer pH, base pairs, and relative orientations of 5-HC and the dimer within the strands. Intrastrand electron transfer repair of dimer by 5-HC is found less efficient than interstrand repair. We explain this result based on the finding in thermal denaturation studies that there exists a low stability structure in dsDNA when 5-HC is flanking the dimer. Except for this discrepancy with a previously report, we find excess electron transfer in our system is preferred: 1) from 3' to 5' when there is one base intervening 5-HC and dimer; 2) from 5' to 3' when 5-HC directly flanks the dimer from the complementary strand; 3) intrastrand is generally preferred compared to interstrand. We also find excess electron transfer in ssDNA has a preference from 3' to 5', irrespective of the distance between 5-HC and dimer. The relevancy of a prebiotic redox cofactor role of 5-HC requires that it

also repair a uracil dimer in RNA. However, we expect that it will repair the uracil dimer with less efficiency due to even poorer base stacking in dsRNA as shown in a previously report (*19*).

Experimental

Oligodeoxynucleotide synthesis and purification. Oligodeoxynucleotides were synthesized at the DNA/Peptide Core Facility at the University of Utah using phosphoramidites purchased from Glen Research. For 5-hydroxy dU containing oligomers, UltraMILD conditions, concentrated ammonium hydroxide 3 h at room temperature, was used to deprotect and cleave the oligomer from the solid support. For 5-hydroxy dC containing oligomers, Mild conditions, concentrated ammonium hydroxide 36 h at room temperature, were used to deprotect and cleave the oligomer from the solid support. For 8-amino dG and 2-amino dA containing oligomers, manufacture recommended conditions were used for deprotection. For *cis*, *syn*-thymine dimer containing oligomers, literature method was used without modification (*19*). In the case where both 5-hydroxyl dC and *cis*, *syn*-thymine dimer are present in the oligomers, mild conditions were used. Crude oligomers were purified by HPLC on a Dionex DNA Pac PA-100 column with linear gradient of 15% B to 100% B over 30 min (Solvent A: 10% acetonitrile in water; solvent B: 1.5 M sodium acetate, 10% acetonitrile in water, pH 7). Oligomers were then dialysed against water for 36 h at 4°C in the dark. The purity and identity of oligomers were determined by analytical HPLC and mass spectrometry.

T$_m$ measurement. 2 μM of each strand in buffer (20 mM sodium borate, 100 mM NaCl, pH 8.5) were annealed by heating to 90 °C for 1 min, then slowly cooled down to room

temperature. Thermal melting experiments were carried out on a Shimadzu UV-1800 UV-VIS spectrophotometer by measuring the change in absorbance at 260 nm from 80 °C to 20 °C at a rate of 1 °C/min. The reverse temperature traces were measured under the same conditions to confirm the reversibility of the annealing process. The melting temperatures were determined from the maximum in the first derivatives of the melting curves using OriginLab software (version 8.5).

Photorepair of *cis, syn*-thymine dimer in DNA duplexes. For pH dependent studies, sodium borate was used to prepare buffers with pH 7.5, 8.0, 8.5, and 9.0; ethanolamine buffer was used for buffer with pH 9.5; sodium phosphate buffer was used for a buffer at pH 7.0. 5 μM of thymine dimer containing DNA was annealed with 1.3 equiv. of the corresponding complementary strand in an appropriate buffer solution by heating at 90 °C for 1 min and slowly cooling to room temperature. The reaction and analysis conditions are the same as previously reported (*19*).

Photorepair of *cis, syn*-thymine dimer in ssDNA. This part is the same as previously reported without modification (*19*).

References

1. Gilbert, W. (1986) Origin of life: The RNA world, *Nature 319*, 618-618.

2. Zhang, B., and Cech, T. R. (1997) Peptide bond formation by in vitro selected ribozymes, *Nature 390*, 96-100.

3. Unrau, P. J., and Bartel, D. P. (1998) RNA-catalysed nucleotide synthesis, *Nature 395*, 260-263.

4. Tsukiji, S., Pattnaik, S. B., and Suga, H. (2003) An alcohol dehydrogenase ribozyme, *Nat. Struct. Biol. 10*, 713-717.

5. Rogers, J., and Joyce, G. F. (1999) A ribozyme that lacks cytidine, *Nature 402*, 323-325.

6. Reader, J. S., and Joyce, G. F. (2002) A ribozyme composed of only two different nucleotides, *Nature 420*, 841-844.

7. Johnston, W. K., Unrau, P. J., Lawrence, M. S., Glasner, M. E., and Bartel, D. P. (2001) RNA-catalyzed RNA polymerization: accurate and general RNA-templated primer extension, *Science 292*, 1319-1325.

8. Illangasekare, M., and Yarus, M. (2012) Small aminoacyl transfer centers at GU within a larger RNA, *RNA Biol 9*.

9. Nissen, P., Hansen, J., Ban, N., Moore, P. B., and Steitz, T. A. (2000) The structural basis of ribosome activity in peptide bond synthesis, *Science 289*, 920-930.

10. Cockell, C. S. (2000) Ultraviolet radiation and the photobiology of earth's early oceans, *Orig. Life Evol. Biosph. 30*, 467-499.

11. Even though it is widely believed that the primordial earth is most likely anoxic, oxidation reaction is still possible. It has been proposed that on the "Snowball Earth", freeze-thaw cycles coupled with photolysis process could have generated sufficient H_2O_2 (see ref. 12), which are an important reagent in Fenton chemistry. Together with Fe(II) and Cu(I), an even more reactive HO radical could be generated.

12. Liang, M. C., Hartman, H., Kopp, R. E., Kirschvink, J. L., and Yung, Y. L. (2006) Production of hydrogen peroxide in the atmosphere of a Snowball Earth and the origin of oxygenic photosynthesis, *Proc. Natl. Acad. Sci. U.S.A. 103*, 18896-18899.

13. Nguyen, K. V., and Burrows, C. J. (2012) Whence flavins? Redox-active ribonucleotides link metabolism and genome repair to the RNA world, *Acc. Chem. Res. 45*, 2151-2159.

14.   Yarus, M. (2011) Getting past the RNA world: the initial Darwinian ancestor, *Cold Spring Harb. Perspect. Biol. 3*.

15.   Wagner, J. R., Hu, C. C., and Ames, B. N. (1992) Endogenous oxidative damage of deoxycytidine in DNA, *Proc. Natl. Acad. Sci. U.S.A. 89*, 3380-3384.

16.   Yanagawa, H., Ogawa, Y., Ueno, M., Sasaki, K., and Sato, T. (1990) A novel minimum ribozyme with oxidoreduction activity, *Biochemistry 29*, 10585-10589.

17.   Havelund, J. F., Giessing, A. M., Hansen, T., Rasmussen, A., Scott, L. G., and Kirpekar, F. (2011) Identification of 5-hydroxycytidine at position 2501 concludes characterization of modified nucleotides in E. coli 23S rRNA, *J. Mol. Biol. 411*, 529-536.

18.   Yanagawa, H., Ogawa, Y., and Ueno, M. (1992) Redox ribonucleosides. Isolation and characterization of 5-hydroxyuridine, 8-hydroxyguanosine, and 8-hydroxyadenosine from Torula yeast RNA, *J. Biol. Chem. 267*, 13320-13326.

19.   Nguyen, K. V., and Burrows, C. J. (2011) A prebiotic role for 8-oxoguanosine as a flavin mimic in pyrimidine dimer photorepair, *J. Am. Chem. Soc. 133*, 14586-14589.

20.   Nguyen, K. V., and Burrows, C. J. (2012) Photorepair of cyclobutane pyrimidine dimers by 8-oxopurine nucleosides, *J. Phys. Org. Chem. 25*, 574-577.

21.   Kundu, L. M., Linne, U., Marahiel, M., and Carell, T. (2004) RNA is more UV resistant than DNA: the formation of UV-induced DNA lesions is strongly sequence and conformation dependent, *Chem. Eur. J. 10*, 5697-5705.

22.   Holman, M. R., Ito, T., and Rokita, S. E. (2007) Self-repair of thymine dimer in duplex DNA, *J. Am. Chem. Soc. 129*, 6-7.

23.   Cannistraro, V. J., and Taylor, J. S. (2009) Acceleration of 5-methylcytosine deamination in cyclobutane dimers by G and its implications for UV-induced C-to-T mutation hotspots, *J. Mol. Biol. 392*, 1145-1157.

24.   Pan, Z., Hariharan, M., Arkin, J. D., Jalilov, A. S., McCullagh, M., Schatz, G. C., and Lewis, F. D. (2011) Electron donor-acceptor interactions with flanking purines influence the efficiency of thymine photodimerization, *J. Am. Chem. Soc. 133*, 20793-20798.

25.   Pan, Z., Chen, J., Schreier, W. J., Kohler, B., and Lewis, F. D. (2012) Thymine dimer photoreversal in purine-containing trinucleotides, *J. Phys. Chem. B 116*, 698-704.

26.   Neelakandan, P. P., Pan, Z., Hariharan, M., and Lewis, F. D. (2012) Facially-selective thymine-thymine photodimerization in TTT triads, *Photochem. Photobiol. Sci. 11*, 889-892.

27.   Bourre, F., Renault, G., Seawell, P. C., and Sarasin, A. (1985) Distribution of ultraviolet-induced lesions in simian virus 40 DNA, *Biochimie 67*, 293-299.

28.   Assuming the oxidation potential of 5-HOdC is 0.78 V, the reduction potential of thymine dimer is -1.96 V, and 4.26 eV as the E_{00} excitation energy corresponding to 291 nm excitation energy, substitution of these values into Rehm-Weller equation results in ΔG_{ct}=-1.52 eV.

29.   Zahn, K. E., Averill, A., Wallace, S. S., and Doublie, S. (2011) The miscoding potential of 5-hydroxycytosine arises due to template instability in the replicative polymerase active site, *Biochemistry 50*, 10350-10358.

30.   Park, H., Zhang, K., Ren, Y., Nadji, S., Sinha, N., Taylor, J. S., and Kang, C. (2002) Crystal structure of a DNA decamer containing a cis-syn thymine dimer, *Proc. Natl. Acad. Sci. U.S.A. 99*, 15965-15970.

31.   McAteer, K., Jing, Y., Kao, J., Taylor, J. S., and Kennedy, M. A. (1998) Solution-state structure of a DNA dodecamer duplex containing a Cis-syn thymine cyclobutane dimer, the major UV photoproduct of DNA, *J. Mol. Biol. 282*, 1013-1032.

32.   Lee, J. H., Choi, Y. J., and Choi, B. S. (2000) Solution structure of the DNA decamer duplex containing a 3'-T x T basepair of the cis-syn cyclobutane pyrimidine dimer: implication for the mutagenic property of the cis-syn dimer, *Nucleic Acids Res. 28*, 1794-1801.

33.   Kupfer, P. A., and Leumann, C. J. (2011) Synthesis, base pairing properties and trans-lesion synthesis by reverse transcriptases of oligoribonucleotides containing the oxidatively damaged base 5-hydroxycytidine, *Nucleic Acids Res. 39*, 9422-9432.

34.   Thiviyanathan, V., Somasunderam, A., Volk, D. E., Hazra, T. K., Mitra, S., and Gorenstein, D. G. (2008) Base-pairing properties of the oxidized cytosine derivative, 5-hydroxy uracil, *Biochem. Biophys. Res. Commun. 366*, 752-757.

35.   Thiviyanathan, V., Somasunderam, A., Volk, D. E., and Gorenstein, D. G. (2005) 5-hydroxyuracil can form stable base pairs with all four bases in a DNA duplex, *Chem. Commun.*, 400-402.

36.   Volk, D. E., Thiviyanathan, V., Somasunderam, A., and Gorenstein, D. G. (2006) Ab initio base-pairing energies of uracil and 5-hydroxyuracil with standard DNA bases at the BSSE-free DFT and MP2 theory levels, *Org. Biomol. Chem. 4*, 1741-1745.

37. Cui, S., Kim, Y. H., Jin, C. H., Kim, S. K., Rhee, M. H., Kwon, O. S., and Moon, B. J. (2009) Synthesis and base pairing properties of DNA-RNA heteroduplex containing 5-hydroxyuridine, *BMB Rep. 42*, 373-379.

38. La Francois, C. J., Jang, Y. H., Cagin, T., Goddard, W. A., 3rd, and Sowers, L. C. (2000) Conformation and proton configuration of pyrimidine deoxynucleoside oxidation damage products in water, *Chem. Res. Toxicol. 13*, 462-470.

39. Suen, W., Spiro, T. G., Sowers, L. C., and Fresco, J. R. (1999) Identification by UV resonance Raman spectroscopy of an imino tautomer of 5-hydroxy-2'-deoxycytidine, a powerful base analog transition mutagen with a much higher unfavored tautomer frequency than that of the natural residue 2'-deoxycytidine, *Proc. Natl. Acad. Sci. U.S.A. 96*, 4500-4505.

40. Crespo-Hernandez, C. E., Cohen, B., and Kohler, B. (2005) Base stacking controls excited-state dynamics in A.T DNA, *Nature 436*, 1141-1144.

41. Chen, J., and Kohler, B. (2014) Base stacking in adenosine dimers revealed by femtosecond transient absorption spectroscopy, *J. Am. Chem. Soc. 136*, 6362-6372.

42. Fazio, D., Trindler, C., Heil, K., Chatgilialoglu, C., and Carell, T. (2011) Investigation of excess-electron transfer in DNA double-duplex systems allows estimation of absolute excess-electron transfer and CPD cleavage rates, *Chem. Eur. J. 17*, 206-212.

43. O'Neill, M. A., and Barton, J. K. (2002) Effects of strand and directional asymmetry on base-base coupling and charge transfer in double-helical DNA, *Proc. Natl. Acad. Sci. U.S.A. 99*, 16543-16550.

44. Ito, T., and Rokita, S. E. (2004) Criteria for efficient transport of excess electrons in DNA, *Angew. Chem. Int. Ed. 43*, 1839-1842.

45. Tanaka, M., Elias, B., and Barton, J. K. (2010) DNA-mediated electron transfer in naphthalene-modified oligonucleotides, *J. Org. Chem. 75*, 2423-2428.

46. Ganguly, M., Szulik, M. W., Donahue, P. S., Clancy, K., Stone, M. P., and Gold, B. (2012) Thermodynamic signature of DNA damage: characterization of DNA with a 5-hydroxy-2'-deoxycytidine.2'-deoxyguanosine base pair, *Biochemistry 51*, 2018-2027.

47. O'Neill, M. A., Dohno, C., and Barton, J. K. (2004) Direct chemical evidence for charge transfer between photoexcited 2-aminopurine and guanine in duplex DNA, *J. Am. Chem. Soc. 126*, 1316-1317.

48.   Takaya, T., Su, C., de La Harpe, K., Crespo-Hernandez, C. E., and Kohler, B. (2008) UV excitation of single DNA and RNA strands produces high yields of exciplex states between two stacked bases, *Proc. Natl. Acad. Sci. U.S.A. 105*, 10285-10290.

49.   de La Harpe, K., and Kohler, B. (2011) Observation of Long-Lived Excited States in DNA Oligonucleotides with Significant Base Sequence Disorder, *J. Phys. Chem. Lett. 2*, 133-138.

50.   Su, C., Middleton, C. T., and Kohler, B. (2012) Base-stacking disorder and excited-state dynamics in single-stranded adenine homo-oligonucleotides, *J. Phys. Chem. B 116*, 10266-10274.

51.   Zhang, Y., Dood, J., Beckstead, A. A., Li, X. B., Nguyen, K. V., Burrows, C. J., Improta, R., and Kohler, B. (2014) Efficient UV-induced charge separation and recombination in an 8-oxoguanine-containing dinucleotide, *Proc. Natl. Acad. Sci. U.S.A. 111*, 11612-11617.

52.   Behrens, C., Burgdorf, L. T., Schwogler, A., and Carell, T. (2002) Weak distance dependence of excess electron transfer in DNA, *Angew. Chem. Int. Ed. 41*, 1763-1766.

53.   Ito, T., and Rokita, S. E. (2003) Excess electron transfer from an internally conjugated aromatic amine to 5-bromo-2'-deoxyuridine in DNA, *J. Am. Chem. Soc. 125*, 11480-11481.

54.   Callahan, M. P., Smith, K. E., Cleaves, H. J., 2nd, Ruzicka, J., Stern, J. C., Glavin, D. P., House, C. H., and Dworkin, J. P. (2011) Carbonaceous meteorites contain a wide range of extraterrestrial nucleobases, *Proc. Natl. Acad. Sci. U.S.A. 108*, 13995-13998.

55.   Santhosh, C., and Mishra, P. C. (1991) Electronic spectra of 2-aminopurine and 2,6-diaminopurine: phototautomerism and fluorescence reabsorption, *Spectrochim. Acta A 47*, 1685-1693.

56.   Kawai, K., Kodera, H., and Majima, T. (2010) Long-range charge transfer through DNA by replacing adenine with diaminopurine, *J. Am. Chem. Soc. 132*, 627-630.

57.   Gengeliczki, Z., Callahan, M. P., Svadlenak, N., Pongor, C. I., Sztaray, B., Meerts, L., Nachtigallova, D., Hobza, P., Barbatti, M., Lischka, H., and de Vries, M. S. (2010) Effect of substituents on the excited-state dynamics of the modified DNA bases 2,4-diaminopyrimidine and 2,6-diaminopurine, *Phys. Chem. Chem. Phys. 12*, 5375-5388.

58.   Sawa, T., Zaki, M. H., Okamoto, T., Akuta, T., Tokutomi, Y., Kim-Mitsuyama, S., Ihara, H., Kobayashi, A., Yamamoto, M., Fujii, S., Arimoto, H., and Akaike, T.

(2007) Protein S-guanylation by the biological signal 8-nitroguanosine 3',5'-cyclic monophosphate, *Nat. Chem. Biol. 3*, 727-735.

59.   Sodum, R. S., and Fiala, E. S. (2001) Analysis of peroxynitrite reactions with guanine, xanthine, and adenine nucleosides by high-pressure liquid chromatography with electrochemical detection: C8-nitration and -oxidation, *Chem. Res. Toxicol. 14*, 438-450.

60.   Sieradzan, I., Marchaj, M., Anusiewicz, I., Skurski, P., and Simons, J. (2014) Prediction of thymine dimer repair by electron transfer from photoexcited 8-aminoguanine or its deprotonated anion, *J. Phys. Chem. A 118*, 7194-7200.

61.   Sodum, R. S., Nie, G., and Fiala, E. S. (1993) 8-Aminoguanine: a base modification produced in rat liver nucleic acids by the hepatocarcinogen 2-nitropropane, *Chem. Res. Toxicol. 6*, 269-276.

62.   Venkatarangan, L., Sivaprasad, A., Johnson, F., and Basu, A. K. (2001) Site-specifically located 8-amino-2'-deoxyguanosine: thermodynamic stability and mutagenic properties in Escherichia coli, *Nucleic Acids Res. 29*, 1458-1463.

CHAPTER 3

8-OXO-7,8-DIHYDROGUANOSINE INTERCALATION REPAIR

THYMINE DIMER IN DUPLEX

Introduction

Due to the lack of ozone layer protection, early genomes of the proposed RNA world

(*1*) are thought to have been under a significant amount of stress from UV irradiation. How

did the early RNA genome manage to protect its integrity from deleterious UV damage?

For example, thymine dimers, if left unrepaired, could lead to abnormal genome replication.

In present-day organisms, this is mitigated by photolyase that can reverse a thymine dimer

into two thymines by recruiting a redox cofactor flavin (*2*) and restore normal genome

replication. Interestingly, the protein itself does not contribute to the repair activity but acts

as a binding scaffold to hold the flavin and the DNA substrate in place. This protein-based

scaffold has been shown to be replaceable by RNA. For example, *in vitro* selection method

has demonstrated that an RNA aptamer can also bind to flavin (*3, 4*), and the binding

complex can even be utilized in redox reactions (*5, 6*). In all, these experiments raise the

possibility of flavin-mediated ribozyme-catalyzed photorepair in the primordial Earth. A

recent report of a thiamin-utilizing ribozyme further supports this hypothesis (*7, 8*). Along

this line, one may further ask if the protein-based scaffold is replaceable, then what about

the flavin cofactor? Are there other redox molecules that predate flavin in the hypothesized

RNA world?

8-Oxo-7,8-dihydroguanosine (O) was previously proposed as a primitive flavin surrogate in RNA-based photocatalysis (*9*). It has been demonstrated that a thymine dimer could be repaired by either free O nucleoside (*10*) or covalently linked O in an oligomer (*11*). Even though the atmosphere of primordial Earth might be largely reductive or neutral, oxidative species, such as H_2O_2, can still exist via photolysis of H_2O (*12*). Thus, we hypothesized that free O might be readily available from G via Fenton chemistry. Abundant free floating O serves as a target ligand for natural evolution to take place on the ample ribozyme pools. Some of the ribozymes may stand out that show strong binding affinity to O nucleoside (O nucleoside-binding DNA (*13*) and RNA (*14*) aptamers have previously been developed by other laboratories and recently by our laboratory). The Burrows laboratory has already shown that free O nucleoside can repair a thymine dimer in the solution. In our continued investigation of O redox chemistry, we further hypothesize that an O nucleoside or nucleobase could have better catalytic activity by binding with a ribozyme that functions as a scaffold mimicking an active photolyase.

Abasic sites (apurinic or apyrimidinic sites; AP sites) can be formed by spontaneous hydrolysis of the N-glycosidic bonds of the nucleotides or during enzymatic repair of damaged DNA nucleobases by the base excision repair mechanism. It is estimated that more than 10,500 AP sites can be generated under physiological conditions in a cell daily (*15*). Left unrepaired, they could lead to mutations or cell death. AP sites may have been quite abundant in the early RNA world due to the existence of various modified RNA bases which might tend to have a labile N-glycosidic bond (*16, 17, 18*). The cleavage of nucleobases from the backbone leaves a cavity, a space that is big enough to allow suitable

structures to stack inside the helix. A plethora of small molecules (*19, 20, 21, 22*), including O free base (*23, 24*), has previous been inserted into an AP site. The interaction between the AP site and the inserted molecule typically includes hydrogen bonding, aromatic interactions, and structural complementarity which are commonly found in the *in vitro* evolved substrate-binding ribozymes. Thus, we envisioned the AP site in the DNA duplex as a minimal ribozyme model, lending us an opportunity to test the hypothesis. In this chapter, we will explore the possibility of O binding to the AP site, and investigate the parameters that affect thymine dimer repair by the inserted O nucleoside.

Results and discussions

Nguyen (*11*) previously demonstrated that thymine dimer repair by O in duplex context is distance-dependent. No repair was observed if O is located more than two bases away from the thymine dimer. To simplify the analysis of thymine dimer repair, we decided to place an AP site close to the thymine dimer (Figure 3.1). A tetrahydrofuran (F) residue was incorporated instead to provide greater stability of the oligonucleotides towards hydrolysis. Thus, the sequences can be annealed by heating at 90 °C for 2 min, then slowly cooling down to room temperature without any sign of strand breakage due to β-elimination. The thymine dimer strand was designed to be 4 bases shorter than the complementary strand to simplify HPLC analysis on a reversed-phase column, for which the repaired thymine dimer will elute after the thymine dimer strand and before the complementary strand (Figure 3.2).

Previously, the O nucleobase has been inserted into an AP site of a DNA duplex (*23*) and a triplex (*24*). The interaction between O nucleobase and DNA is believed to be via H-bonding. Considering the nucleobase and nucleoside have the same hydrogen bond donor

Figure 3.1 AP site containing DNA sequences. F stands for dSpacer.
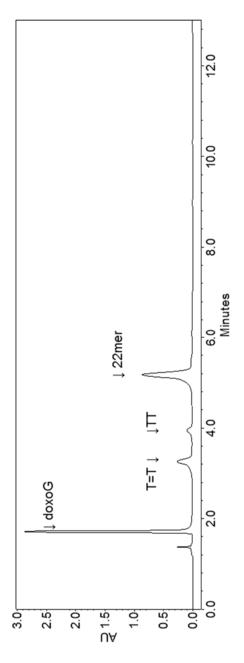
Figure 3.2 Typical UPLC trace showing good separation of thymine dimer strand (3.2 min), repaired thymine dimer strand (4.0 min), and the complementary strand (5.2 min). UPLC condition: flow rate 0.3 mL/min, 8-13% B in 10 min, 0.3 mL/min, A=50 mM TEAA pH 7, B=Acetonitrile, column temperature 65 °C.

and acceptor patterns, we anticipated that the O nucleoside could also be inserted into an AP site of the DNA duplex via hydrogen bonding. To test the hypothesis, we mixed 5 μM annealed sequence **1** and 500 μM O nucleoside and irradiated the solution in a polystyrene cuvette with a UV-B lamp (λ_{max}=313 nm). The polystyrene cuvettes have a wavelength cutoff value below 300 nm; thus it can block light absorption by the DNA strand and focus light >300 nm on the O nucleoside. After 2 h irradiation, we analyzed the sample on a reversed-phase column, and observed a new peak (λ_{max}=260 nm) appearing after the thymine dimer strand peak and before the complementary strand peak, indicating a repaired thymine dimer strand. The new peak is generated in 20% yield. The repair is much more efficient compared to the bimolecular reaction in the previous study (*10*). To exclude the possibility of thymine dimer strand self-repair under UV-B irradiation (*25*), we also irradiated sequence **1** by itself under the same conditions. However, no new peak appeared in between the thymine dimer strand and the complementary strand peaks. This experiment confirms that the thymine dimer is repaired by an inserted O nucleoside. Among the four canonical bases, G is the easiest to oxidize, followed by A whose redox potential is about 130 mV higher than that of G (*26*). In our sequence **1**, A, being high redox potential relative to G, is located on the 5' side of the thymine dimer. Thus, this may explain why no self-repair was observed. To further prove thymine dimer is repaired by an intercalating O nucleoside instead of free floating O nucleoside, we also irradiated sequence **3** and O nucleoside and found no new peak formation in the HPLC trace. In sequence **3**, the O nucleoside cannot insert into the duplex due to the absence of an AP site. Therefore, this control experiment further supports that the thymine dimer is repaired by an intercalating O nucleoside, not by free floating O nucleoside.

The interaction between the O nucleoside and the duplex structure likely involves a wobble base pair with the opposite T and base stacking with surrounding bases (*27*). The formation of a wobble base pair with the opposite T (Figure 3.3) may introduce very little backbone conformation distortion and has little impact on the base stacking with surrounding bases. To support the proposal that H-bonding is responsible for the interaction, we did the repair experiment at 4 °C under which conditions stable O:T wobble base pair is expected. A stable base pair between the O nucleoside and T can lead to strong binding affinity, which in turn results in higher repair yield. We indeed observed an increased repair yield of 27% at 4 °C. Low temperature can also lead to a stable duplex structure with better base stacking which in turn can result in higher repair yield. The melting temperature of sequence **1** is measured to be 50.6 °C (Figure 3.4). Thus, the difference of base stacking under room and low temperature may be only modest and base stacking may have little effect on repair rate. The much more efficient thymine dimer repair by an intercalating O nucleoside compared to the bimolecular reaction may reflect the favorable photophysics of an O nucleoside under the influence of both wobble base pairing and base stacking, which tend to slow down the ultrafast deactivation by forming a charge-transfer state (*28*).

Having established that O nucleoside can bind to an AP site via wobble base pairing with T, we next studied its concentration effect on thymine dimer repair. As a general trend, apurinic site DNA duplex offers a larger binding site than the apyrimidinic site. Thus, purine nucleosides have high binding affinity to AP site containing DNA duplexes with complementary nucleosides opposite the AP site (*29*). Also, the normal Watson-Crick base pair is expected to have a higher binding constant (*23, 24*). We clearly observed a concentration-dependent repair curve (Figure 3.5). It is previously reported that the binding
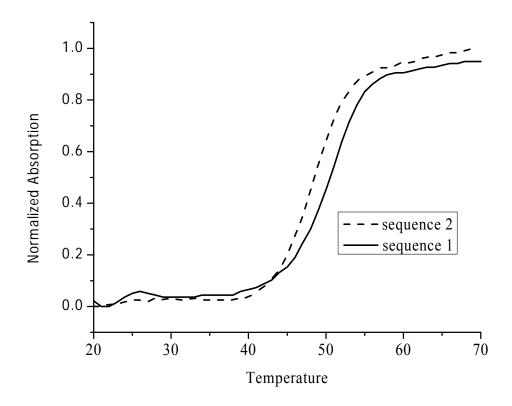
Figure 3.3 Wobble base pair between O and T

Figure 3.4 Melting curve of sequence **1** and **2**.
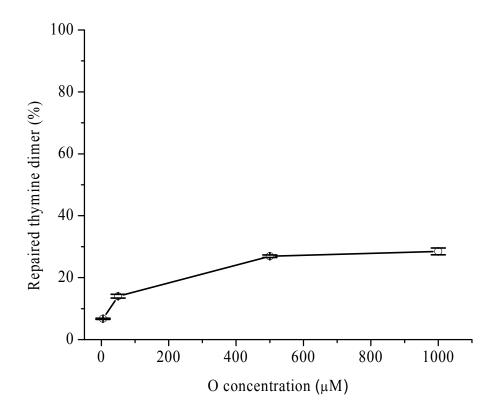
Figure 3.5 Concentration-dependent repair of thymine dimer in DNA duplex

constant K_d of the O nucleobase with an AP site containing DNA aptamer is 5.5 μM (*23*) and 22 nM (*24*) for the O nucleobase with an AP site containing DNA triplex. The binding constant of the O nucleoside with the AP site containing duplex sequence **1** is estimated at low micromolar concentration from the dose-response curve, consistent with the literature value. The exact binding constant K_d could be accurately measured using isothermal calorimetry (ITC). However, we did not pursue this experiment due to the prohibitively large quantity of sample required (at least 200 nmol).

We also attempted to repair thymine dimer from the 5' direction as in sequence **2**. At this position, the O nucleoside is expected to form a Hoogsteen base pair with A. At room temperature, sequence **2** should be relatively stable, as can be seen from its high melting temperature at 47.8 °C (Figure 3.4), though it is 3 °C less than sequence **1**. The binding affinity of the O nucleoside on this AP site may be similar to the one in sequence **1**. The efficiency of repair from this side is 3.5-fold lower. This observation is consistent with earlier results for a covalently attached O nucleoside in DNA duplex. The low repair efficiency from the 5' side likely may reflect the smaller efficiency of charge-transfer state formation between the O nucleoside and the thymine dimer in this orientation.

The thymine dimer repair rate via an intercalating O nucleobase is about the same as by an intercalating O nucleoside. This similar repair efficiency may come from their similar binding affinities to the AP site and their base pairing patterns.

As expected, we have showed that intercalation interaction can indeed increase the binding affinity of small redox-active molecules. Encouraged by this success, we are interested in several flavin-like "prebiotic" molecules (Figure 3.6) synthesized by the group of Nicholas Hud. These two molecules are readily available from a solution-phase conden-

Figure 3.6 Flavin-like molecules.

sation of 5,6-diaminopyrimidines. However, no repaired thymine dimer was detected when irradiating the mixture of AP site containing DNA duplex and these molecules in several conditions including addition of reductant to, hopefully, convert these molecules into an active form in situ. Several factors may contribute to this observation. First, the redox potentials are unknown for these synthetic flavin-like molecules. Thus, they may not be good electron doners. Second, even though similar structures have previously been shown to intercalate into a DNA strand (*30*), it is unknown whether the present set of molecules can intercalate into an AP site. Future work should focus on measuring their redox potentials and improve their solubility. Surprisingly, flavin and some other active flavin-like molecules have substitution on N^{10} position. This substitution can significantly enhance their water solubility and may convert these molecules from redox inactive to active.

Conclusion

In summary, we demonstrated that O nucleoside could bind to an AP site in a DNA duplex, a model of a minimal photolyase-like ribozyme, with reasonably good affinity. The binding affinity is remarkable considering that a Wobble base pair is formed in a locally distorted region due to thymine dimer formation. Upon photo irradiation, thymine dimer in the DNA duplex could be repaired to two thymines by an intercalating O nucleoside, even though the repair yield is not as good as for covalently attached analogs. In this experiment, we show that the thymine dimer repair activity of the flavin mimic can indeed be enhanced by binding to a ribozyme. This ribozyme may function as a binding scaffold to bring the two reactants in proximity. The current AP site containing DNA duplex could

also be used to screen a variety of other prebiotic molecules for their photorepair capability.

Experimental

Materials. All chemicals used in this chapter were purchased from commercial sources and used without further purification except where otherwise mentioned. 8-Oxo-7, 8-dihydroguanosine was purchased from Cayman Chemical (Ann Arbor, MI). 8-Oxo-7, 8-dihydro-2'-deoxyguanosine was purchased from Berry & Associates (Dexter, MI). FAD as disodium salt hydrate was purchased from Sigma-Aldrich. The oligonucleotides were synthesized by the DNA/Peptide Synthesis Core Facility at the University of Utah following standard solid-phase synthetic protocols using commercially available phosphoramidites (Glen Research, Sterling, VA). Thymine dimer containing oligonucleotide was deprotected and purified following previous procedure (*11*).

Thermal analysis of AP site containing DNA duplex. 2 μM DNA duplex was annealed in 20 mM NaPi, 100 mM NaCl pH 7 buffer by heating to 90 °C for 2 min and slowly cooling to room temperature. Thermal melting experiment was carried out in triplicate on a Shimadzu UV-1800 UV-VIS spectrophotometer by monitoring change in absorbance at 260 nm from 20 °C to 90 °C at a rate of 1 °C/min. The reverse temperature trace was measured under the same conditions to confirm the reversibility of the annealing process. The melting temperature T_m was determined from the maximum of the first derivative of the melting curves using OriginLab software (version 8.5).

Photorepair of thymine dimer by O. DNA duplex (5 μM) in 20 mM NaPi, 100 mM NaCl pH 7 buffer was annealed by heating at 90 °C for 2 min, then slowly cooling down to room temperature. The annealed samples were kept at 4 °C before use. An aliquot of

concentrated O was added to the specified concentration before irradiation using an FS40 UVB lamp (λ_{max}=313 nm).

Repair analysis using UPLC. The photo irradiated samples were analyzed by UPLC on a Waters Symmetry C18 column (3.5 μm, 4.6×75 mm) with linear gradient of 8% B to 13% B over 10 min (solvent A: 50 mM TEAA pH 7; solvent B: acetonitrile; flow rate: 0.3 mL/min; column temperature: 65°C). The peaks corresponding to CPD and the repaired CPD were integrated and normalized against extinction coefficients in triplicate to calculate the average repair yield.

References

1.   Gilbert, W. (1986) Origin of life: The RNA world, *Nature 319*, 618-618.

2.   Sancar, A. (2003) Structure and function of DNA photolyase and cryptochrome blue-light photoreceptors, *Chem. Rev. 103*, 2203-2237.

3.   Burgstaller, P., and Famulok, M. (1994) Isolation of RNA aptamers for biological cofactors by in vitro selection, *Angew. Chem. Int. Ed. 33*, 1084-1087.

4.   Lauhon, C. T., and Szostak, J. W. (1995) RNA aptamers that bind flavin and nicotinamide redox cofactors, *J. Am. Chem. Soc. 117*, 1246-1257.

5.   Tsukiji, S., Pattnaik, S. B., and Suga, H. (2003) An alcohol dehydrogenase ribozyme, *Nat. Struct. Biol. 10*, 713-717.

6.   Tsukiji, S., Pattnaik, S. B., and Suga, H. (2004) Reduction of an aldehyde by a NADH/Zn^{2+} -dependent redox active ribozyme, *J. Am. Chem. Soc. 126*, 5044-5045.

7.   Cernak, P., and Sen, D. (2013) A thiamin-utilizing ribozyme decarboxylates a pyruvate-like substrate, *Nat. Chem. 5*, 971-977.

8.   Burrows, C. J. (2013) Prebiotic chemistry: Ribozyme takes its vitamins, *Nat. Chem. 5*, 900-901.

9.   Nguyen, K. V., and Burrows, C. J. (2012) Whence flavins? Redox-active ribonucleotides link metabolism and genome repair to the RNA world, *Acc. Chem. Res. 45*, 2151-2159.

10.   Nguyen, K. V., and Burrows, C. J. (2012) Photorepair of cyclobutane pyrimidine dimers by 8-oxopurine nucleosides, *J. Phys. Org. Chem. 25*, 574-577.

11.   Nguyen, K. V., and Burrows, C. J. (2011) A prebiotic role for 8-oxoguanosine as a flavin mimic in pyrimidine dimer photorepair, *J. Am. Chem. Soc. 133*, 14586-14589.

12.   Liang, M. C., Hartman, H., Kopp, R. E., Kirschvink, J. L., and Yung, Y. L. (2006) Production of hydrogen peroxide in the atmosphere of a Snowball Earth and the origin of oxygenic photosynthesis, *Proc. Natl. Acad. Sci. U.S.A. 103*, 18896-18899.

13.   Miyachi, Y., Shimizu, N., Ogino, C., Fukuda, H., and Kondo, A. (2009) Selection of a DNA aptamer that binds 8-OHdG using GMP-agarose, *Bioorg. Med. Chem. Lett. 19*, 3619-3622.

14.   Rink, S. M., Shen, J. C., and Loeb, L. A. (1998) Creation of RNA molecules that recognize the oxidative lesion 7,8-dihydro-8-hydroxy-2'-deoxyguanosine (8-oxodG) in DNA, *Proc. Natl. Acad. Sci. U.S.A. 95*, 11619-11624.

15. Tropp, B. E. (2011) *Molecular biology*, Jones and Bartlett, Sudbury.

16. Gates, K. S. (2009) An overview of chemical processes that damage cellular DNA: spontaneous hydrolysis, alkylation, and reactions with radicals, *Chem. Res. Toxicol. 22*, 1747-1760.

17. Rios, A. C., and Tor, Y. (2013) On the origin of the canonical nucleobases: an assessment of selection pressures across chemical and early biological evolution, *Isr. J. Chem. 53*, 469-483.

18. Rios, A. C., and Tor, Y. (2012) Refining the genetic alphabet: a late-period selection pressure?, *Astrobiology 12*, 884-891.

19. Nishizawa, S., Sato, Y., and Teramae, N. (2014) Recent progress in abasic site-binding small molecules for detecting single-base mutations in DNA, *Anal. Sci. 30*, 137-142.

20. Campbell, N. P., and Rokita, S. E. (2014) Electron transport in DNA initiated by diaminonaphthalene donors alternatively bound by non-covalent and covalent association, *Org. Biomol. Chem. 12*, 1143-1148.

21. Lhomme, J., Constant, J. F., and Demeunynck, M. (1999) Abasic DNA structure, reactivity, and recognition, *Biopolymers 52*, 65-83.

22. Benner, K., Bergen, A., Ihmels, H., and Pithan, P. M. (2014) Selective stabilization of abasic site-containing DNA by insertion of sterically demanding biaryl ligands, *Chem. Eur. J. 20*, 9883-9887.

23. Roy, J., Chirania, P., Ganguly, S., and Huang, H. (2012) A DNA aptamer sensor for 8-oxo-7,8-dihydroguanine, *Bioorg. Med. Chem. Lett. 22*, 863-867.

24. Zhang, Q., Wang, Y., Meng, X., Dhar, R., and Huang, H. (2013) Triple-stranded DNA containing 8-oxo-7,8-dihydro-2'-deoxyguanosine: implication in the design of selective aptamer sensors for 8-oxo-7,8-dihydroguanine, *Anal. Chem. 85*, 201-207.

25. Holman, M. R., Ito, T., and Rokita, S. E. (2007) Self-repair of thymine dimer in duplex DNA, *J. Am. Chem. Soc. 129*, 6-7.

26. Burrows, C. J., and Muller, J. G. (1998) Oxidative nucleobase modifications leading to strand scission, *Chem. Rev. 98*, 1109-1152.

27. Lee, J. H., Park, C. J., Shin, J. S., Ikegami, T., Akutsu, H., and Choi, B. S. (2004) NMR structure of the DNA decamer duplex containing double T*G mismatches of cis-syn cyclobutane pyrimidine dimer: implications for DNA damage recognition by the XPC-hHR23B complex, *Nucleic Acids Res. 32*, 2474-2481.

28. Zhang, Y., Dood, J., Beckstead, A. A., Li, X. B., Nguyen, K. V., Burrows, C. J., Improta, R., and Kohler, B. (2014) Efficient UV-induced charge separation and recombination in an 8-oxoguanine-containing dinucleotide, *Proc. Natl. Acad. Sci. U.S.A. 111*, 11612-11617.

29. Pang, Y., Xu, Z., Sato, Y., Nishizawa, S., and Teramae, N. (2012) Base pairing at the abasic site in DNA duplexes and its application in adenosine aptasensors, *ChemBioChem 13*, 436-442.

30. Horowitz, E. D., Engelhart, A. E., Chen, M. C., Quarles, K. A., Smith, M. W., Lynn, D. G., and Hud, N. V. (2010) Intercalation as a means to suppress cyclization and promote polymerization of base-pairing oligonucleotides in a prebiotic world, *Proc. Natl. Acad. Sci. U.S.A. 107*, 5288-5293.

CHAPTER 4

EXCITED-STATE DECAY OF 8-OXO-7,8-DIHYDRODEOXYGUANINE

IN NUCLEOSIDE, DINUCLEOTIDE, AND DUPLEX: EFFECT

OF BASE STACKING AND BASE PAIRING

Introduction

Life based on self-replicating RNA molecules has been proposed to exist before DNA-
and protein-based life (*1, 2, 3*). The smoking gun evidence supporting this RNA world
hypothesis (*4*) is probably the finding that the contemporary ribosome active site structure
contains only RNA, no amino acids (*5, 6, 7*). "Fossils of the RNA world (*8*)" could also be
found in extant redox cofactors, such as FAD and NADH: each comprises a ribose unit, a
heterocycle, and an adenosine nucleotide. These redox cofactors can also team up with
ribozymes in redox reactions (*9, 10*). These pieces of evidence can support the RNA world
hypothesis but cannot answer the question of where these cofactors came from. Could they
have been synthesized in the primordial soup based on plausible reactions from small
molecules in a fashion similar to prebiotic routes to purines and pyrimidines (*11, 12*) or did
they evolve from existing purines and pyrimidines into redox-active derivatives and finally
present-day cofactors?

The Burrows laboratory recently showed a common purine derivative from oxidation,
8-oxo-7,8-dihydroguanine (O), can photo-repair thymine dimers (*13, 14, 15*). This led to

the hypothesis that O may have functioned as a primitive flavin. Analogous to flavin in photolyase, O is also an excellent electron donor upon incident long wavelength light. The repair of thymine dimer in an O-containing DNA duplex is proposed to follow an excess electron transfer (EET) mechanism and found to be dependent on many factors. For example, it is shown that the O:C base pair has a lower repair activity than the O:A base pair (*13*). It is proposed that proton-coupled electron transfer (PCET) may quickly deactivate the excited-state of O:C base pair, thus making excess electron transfer (EET) repair of thymine dimer inefficient. This mechanism was later supported by a computational study (*16*). To get direct experimental evidence that the excited-state lifetime of O:C base pair is shorter than that of the O:A base pair, we decided to measure their excited-state lifetime using femtosecond transient-absorption spectroscopy technique by collaborating with researchers at Montana State University (Bozeman, MT).

The excited-state decay of O nucleoside is most likely context-dependent as observed previously in studies with the canonical bases (*17*). To dissect how the O nucleoside behaves in a more complex DNA duplex, we isolated possible determining factors and studied them separately. This chapter is thus divided into three sections. We begin the first section with studying the excited-state dynamics of the simple O nucleoside in solution. In the second section, we consider possible base-stacking effects on the O nucleoside excited-state decay by studying an O-containing dinucleotide. In the final section, we will examine a more complex system, an O-containing minicircle molecule that has only two base pairs. We will discuss our effects on synthesizing the minicircles. The minicircle molecule is constructed as a minimal model of a DNA duplex featuring both base pair and base stacking effects.

Results and discussion

8-oxo-7,8-dihydroguanine nucleoside. DNA bases are enduring constant UV assault. However, the extent of photodamage is remarkably lower than expected. Previously, it has been shown that excited-states of the common DNA bases decay in the hundreds of femtoseconds via internal conversion to their electronic ground states (*18*). This ultrafast nonradiative decay is proposed as an important molecular survival mechanism to mitigate the damage and may also have played an important role in the evolution of life (*19*). The excited-state lifetime of the O nucleoside was proposed to play a significant role in thymine dimer repair. However, the excited-state dynamics of O nucleoside is presently unknown. We provided the O nucleoside sample to the Montana group led by Prof. Bern Kohler to initiate the study of its excited-state dynamics.

The O nucleoside is an excellent electron donor that can be easily oxidized via chemical and photochemical methods. The oxidation product is dependent on the context (*20*) and also pH of the solution (*21*). Under slightly basic conditions, the O nucleoside exists in both neutral and anionic forms. Thus, its excited-state lifetime was measured in both neutral and basic conditions to better understand its photo-dynamical behavior. UV pump/visible probe experiments were carried out to measure its excited-state lifetimes. Under neutral conditions, after 267 nm excitation, the 570 nm transient is well fit by a single exponential with a time constant of 0.9 ps (Figure 4.1), corresponding to the lifetime of the lowest excited-state supported by computational study (*22*). Interestingly, this excited-state lifetime is about twice as long as the G nucleoside. However, under basic conditions, a much longer excited-state lifetime of 43 ps is observed. The repopulation of the ground state anionic O nucleoside is about 50 times slower than that for the neutral
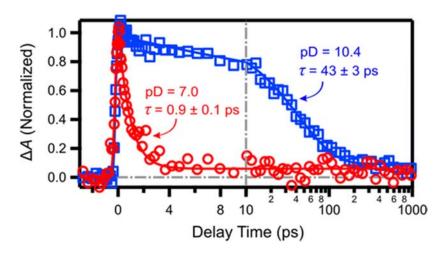
Figure 4.1 Kinetic traces showing excited-state absorption (ESA) for a probe wavelength of 570 and 267 nm excitation. Red circles: 1 mM 8-oxodG at pD = 7.0; blue squares: 1 mM 8-oxodG at pD = 10.4. The signals have been corrected for solvated electrons. The solid curves are best fits to the data points. The exponential functions are convoluted with an instrument response function (IRF) of 380 fs. *Reprinted with permission from Zhang et al. (22). Copyright 2013 American Chemical Society.*

form of the O nucleoside. This long excited-state lifetime of the O nucleoside under basic conditions may explain its 30-fold more efficient ET thymine dimer repair activity compared to the short-lived neutral O nucleoside (*14*) though we cannot currently assess the effect of other factors, for example, rates of forward ET to T=T and back ET from T=T to the O nucleoside. Overall, ultrafast nonradiative decay of the O nucleoside, compared to the 1.3 ns excited-state lifetime of $FADH^-$ in photolyase, can lead to a high degree of photostability, which is probably beneficial to the integrity of genome and is hypothesized to be one of the selection pressures for the canonical bases (*19*). However, the ability of the O nucleoside to efficiently undergo nonradiative decay is contradictory to its ability of photo-induced electron transfer repairing thymine dimer. The deactivation pathway may be quite different in the presence of base pairing and base stacking. Thus, it warrants further investigation of the O nucleoside excited-state dynamics in a more complex system.

8-oxo-7,8-dihydroguanine dinucleotide: d(OA) and d(AO). The Kohler group has previously studied excited-state dynamics of various dinucleotides (*23*). In their experiment, they observed a one or two orders of magnitude longer excited-state lifetime than those of equimolar mixtures of nucleosides, indicating a charge transfer (CT) state between the stacked bases in dinucleotides. However, there is no direct experimental evidence to support a CT state. The d(OA) dinucleotide was previously chosen as a crude mimic of $FADH_2$ in which O replaces the dihydroflavin moiety of the cofactor that has been shown to serve as the electron source for photo-initiated ET to thymine dimer. A further difference is that the d(OA) dinucleotide is linked by a single 3'-5' phosphodiester bond, as opposed to the 5'-5' diphosphate linkage of $FADH_2$. Rapid nonradiative decay of the O nucleoside as has been shown in the previous section could make dOA a poor electron

donor despite its favorable thermodynamics. To study how the O nucleoside gets around this rapid nonradiative decay in the dinucleotide context and how base stacking could affect its photophysics, we studied the decay of the dOA dinucleotide following UV excitation. To assess the contribution of each individual base and circumvent the drawback of ambiguity inherited in the UV/Vis probe experiment, we followed the decay using femtosecond time-resolved infrared (TRIR) spectroscopy as it can detect and differentiate any short-lived radicals produced by photo-induced ET by monitoring the narrow and characteristic nonoverlapping absorption bands displayed by nucleobases in the mid-IR region.

To obtain large quantities of the dinucleotide suitable for the TRIR study at low cost, solution phase synthesis was performed following a literature procedure (*24*). Commercially available 5'-*O*-dimethoxytrityl-*N*^{6}-benzoyldeoxyadenosine **1** was first protected at the 3'-OH with a bulky hydrophobic group to facilitate late stage aqueous extraction (Figure 4.2). Next, the 5'-DMT protecting group was removed in acidic conditions to expose the 5'-OH group. Next, compound **3** was activated using dicyanoimidazole (DCI), coupled with the O phosphoramidite, and oxidized using I_2 solution. The dinucleotide d(OA) **4** was finally deprotected using concentrated ammonium hydroxide and purified on HPLC. For dinucleotide d(AO) **10**, commercially available 5'-*O*-dimethoxytrityl-8-oxo-*N*^{2}-isobutyryl-deoxyguanosine **5** was also protected at the 3'-OH with a bulky hydrophobic group; however, overprotection at the N^1 position generating compound **7** together with compound **6** was observed. The DMT group on the 5'-OH of compounds **6** and **7** could be removed under acidic conditions to give compounds **8** and **9**. Dinucleotide d(AO) **10** was synthesized and purified using the same method as before from

Figure 4.2 Synthesis of the dinucleotide d(OA).

9 and the commercially available dA phosphoramidite (Figure 4.3). The extra protecting group on N^7 has little effect on the coupling yield and can be easily removed using the standard deprotection method. The purity of the dinucleotides d(OA) and d(AO) synthesized was verified on UPLC (Figure 4.4) and their identities were established using high resolution mass spectrometry (HRMS). The distinct absorption peak of the O nucleoside at long wavelength can be observed at 295 nm for both dinucleotides. The characteristic peaks in the mid-IR region corresponding to A and O nucleosides are well resolved (Figure 4.5) and assigned based on a computational study (*25*).

The dinucleotide could also be made using manual solid-phase synthesis to reduce the turnaround time, cut cost, and achieve high yield. Depending on the sequence, the synthesis starts with a column with or without the first base. After deblocking the DMT protecting group, the second base or the first base was activated and coupled with the free hydroxyl group. The phosphite group was oxidized using iodine to a more stable phosphate group. Finally, the DMT group on the newly added base was removed to finalize the synthesis or prepare for the next base addition. The synthesized dinucleotide was cleaved from the support and deprotected using concentrated ammonium hydroxide. Compared to the solution phase synthesis method, the manual solid phase synthesis methodology significantly reduced the turnaround time, saved expensive phosphoramidite, and achieved high yield (40-50% purification yield).

The TRIR experiment done on the synthesized dinucleotides by our collaborators at Montana State showed strong bleaching at the frequencies of the highest peaks in the steady state FTIR absorption spectrum of d(OA); these could be observed after 265 and 295 nm excitation (Figure 4.6). Two exponential time constants, 4 and 60 ps, could be used to

Figure 4.3 Synthesis of the dinucleotide d(AO).

Figure 4.4 Purity of synthesized dinucleotide.
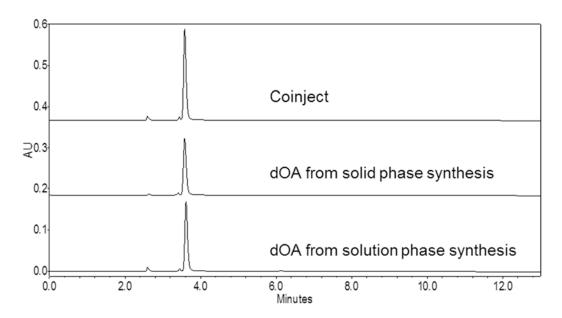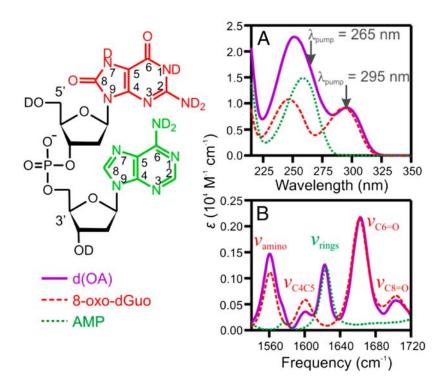
Figure 4.5 UV-visible (A) and FTIR spectra (B) for d(OA) at neutral pH. The spectra of monomeric 8-oxo-dGuo (red dashed curves) and AMP (green dotted curves) are shown for comparison. The excitation wavelengths used in the pump-probe experiments are indicated in A by arrows. *Reprinted with permission from Zhang et al. (25). Copyright 2014 National Academy of Sciences, USA.*

globally fit the measured TRIR spectra. Target and global analysis, backed up by computational study done by another collaborator in Naples, Italy (Roberto Improta and coworkers), unambiguously determine the long-lived transient species at both 265 and 295 nm excitation as the charge transfer state between O and A, forming $O^{\bullet+}A^{\bullet-}$ radical pairs. ET from O to A is remarkably efficient at both wavelength excitations, 0.4 at 265 nm pump and 0.1 at 295 nm pump, indicating a significant amount of base stacking between these two bases. The efficient CT state formation photo initiated at wavelengths used previously between O and A attests to the validity of reductive thymine dimer repair by excited O in a photolyase-like manner.

Thymine dimer repair by the deprotonated O nucleoside shows an elevated repair yield, indicating efficient ET from O^- (*14*). To study the photophysics of O^-A, we also investigated its decay following photoexcitation using TRIR spectra (*26*). Target and global analysis detected a new transient species decaying on a time scale of 9 ps (Figure 4.7). Under basic conditions, much higher quantum yields of approximately unity at 265 nm and 0.85 at 295 nm were observed. The high quantum yield corroborates the validity of the more efficient reductive thymine dimer repair by excited O^- and agrees with experimental observations of a higher repair yield under basic conditions in the O nucleoside studies of repairing a thymine dimer. However, the fast back ET from $A^{\bullet-}$ can directly compete with thymine dimer C_6-$C_{6'}$ bond cleavage, which has been shown to take several hundred picoseconds in a flavin-CPD model or 90 ps in photolyase and to be the rate-determining step in thymine dimer cyclobutane ring cleavage (*27, 28*). This fast back ET may account for the small repair quantum yield by the O nucleoside in thymine dimer repair.
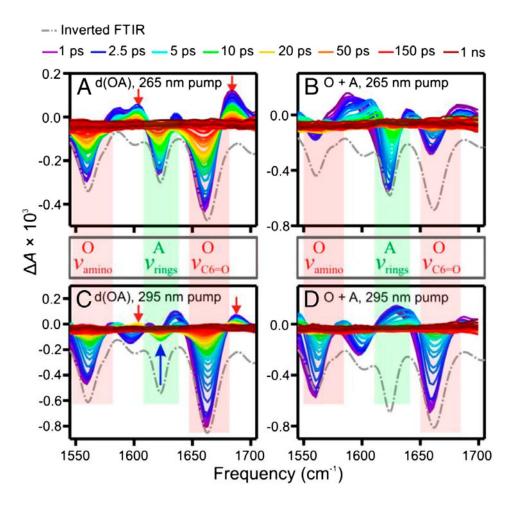
Figure 4.6 TRIR spectra at the indicated pump-probe delay times from a 5 mM solution of the d(OA) dinucleotide (*A* and *C*) and 5 mM 8-oxo-dGuo (O) + 5 mM AMP (A) mixture (*B* and *D*) following 265 nm (*A* and *B*) and 295 nm (*C* and *D*) excitation. Red arrows point to positive signals assigned to vibrational marker bands of 8-oxo-dGuo$^{•+}$. The inverted and scaled steady-state FTIR spectrum for each sample is shown by the dot-dashed gray line. Vibrational mode assignments are included for convenience. *Reprinted with permission from Zhang et al. (25). Copyright 2014 National Academy of Sciences, USA.*
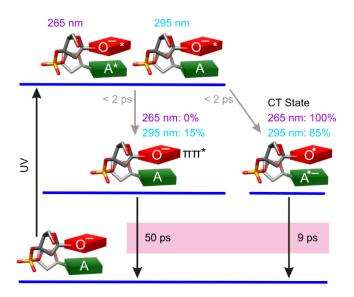
Figure 4.7 Kinetic scheme for d(O⁻A) excited-state dynamics. The relative population of each channel and lifetime obtained from global fitting are indicated. The initial steps, indicated in gray, are faster than our instrument response time. *Reprinted with permission from Zhang et al. (26). Copyright 2015 American Chemical Society.*

Asymmetrical orbital overlap was proposed as the primary factor of directionality of excess electron transfer along DNA (*29*). We also tried to test this hypothesis by investigating the potential EET rate and decay differences between d(OA) and d(AO). However, the EET rate difference could not be substantiated due to the limitation of the instrument resolution of ~500 fs. No significant decay discrepancy between these two dinucleotides was observed.

8-oxo-7,8-dihydroguanine in duplex DNA. In the previous section, we have shown that UV excitation of an O-containing dinucleotide creates a radical ion pair with a lifetime of 60 ps that is unambiguously assigned to interbase CT through the vibrational signature of this state in the double bond stretching region. Thus, the absorbed photon energy is utilized to transport the electron from O to a neighboring stacked base. The following ultrafast charge recombination minimizes the population of reactive radical ions that could, given enough time, lead to decomposition. Thus, base stacking emerges as an important decay channel for the dinucleotide, even for oligonucleotides and duplex, to very quickly dissipate destructive photo energy to nonlethal heat. Carell and Zinth (*30*) proposed through a TRIR experiment on the DNA duplex that Watson-Crick base pairing can also significantly shorten the excited-state lifetime of charge transfer states in natural DNA, signifying another important decay channel for DNA. To investigate how O deactivates in the presence of both base stacking and base pairing and most importantly to study if the proton-coupled electron transfer process operates in an O:C base pair, we decided to study O decay in a duplex that includes both factors.

Even though the absorption bands in the mid-IR region for nuleobases are characteristic (*31*), they can still overlap with each other, especially if multiples of the same nucleobase

exist, thus preventing accurate band assignment. To simplify band assignment for the TRIR spectra, ideally we should work on as short a DNA duplex as possible to minimize band overlap. The minimal unit, including both base pairing and base stacking effects, is a DNA duplex with two base pairs. However, the melting temperature of a typical DNA duplex with only two base pairs would be extremely low, thus preventing the formation of stable base pair under room temperature. Nonetheless, it is well known that connecting one end of a DNA duplex forming a hairpin structure has a stabilizing effect. Along this line, we asked if connecting both ends of the DNA duplex will generate a cyclic duplex that is stable enough under room temperature. Encouraged by a literature report of a stable cyclic miniduplex with only two base pairs (*32*), we decided to move on to synthesize an O-containing cyclic DNA miniduplex, hoping it will also form a stable structure.

We initially opted to avoid the copper-catalyzed alkyne-azide cycloaddition reaction (CuAAC) as was reported in ref (*32*) because it may oxidize the redox sensitive O. Long cyclic DNA duplexes have previously been synthesized using cyanogen bromide (CNBr) (*33*) with polyethylene glycol (PEG) linkers on both ends. The PEG linker will not likely interfere with TRIR experiment in the double bond stretching region. Thus, we designed a nicked dumbbell with a seven base-pair stem to test the feasibility of this method. The ligation was carried out in MES buffer at 0 °C for 5 min. HPLC analysis of the reaction mixture showed that the majority of the nicked dumbbell had been ligated as it eluted faster than the starting material on RP-HPLC column (Figure 4.8A). Encouraged by this result, we next tested this methodology on a short nicked dumbbell with the nick site in the middle of the four base-pair stem (Figure 4.8B). However, only about 40% of the nicked dumbbell was ligated according to HPLC analysis. The decreased ligation yield may reflect the lower

stability of the two base-pair hairpin structure which is expected to melt at less than 29 °C under current conditions (*33*). We also tried to ligate a three base-pair stem (Figure 4.8 C). Not surprisingly, no ligation product was detected in all but one sequence. Two factors may contribute to the extremely low ligation yield. On the one hand, it has been previously shown that the yield of CNBr-mediated ligation of the DNA ends is sensitive to the ligation site sequence (*34*). The extremely low ligation yield may reflect that this sequence is not preferable. On the other hand, in these nicked dumbbells, the structure is expected to be somewhat unstable, thus 3'-phosphate and 5'-OH have a very low chance, if any, to come within van der Waals distance, which is the prerequisite for a successful ligation; otherwise, CNBr will quickly decompose under aqueous conditions. To stabilize the three base-pair stem structure, thus to bring the 3'-phosphate and 5'-OH together, we also tried the ligation under a high salt condition. However, no products were observed.

We next turned our attention back to the original paper that reported the synthesis of a stable cyclic miniduplex. Initially, we followed their procedure synthesized a hairpin DNA with azide and alkyne moieties on one end and PEG linker on the other end (Figure 4.9). However, the DNA decomposed in the final CuAAC reaction in our hands. The DNA CuAAC reaction is notoriously sensitive to the presence of free Cu(I) due to its participation in a Fenton-like reaction which can generate a reactive oxygen species, •HO, from residual O_2 in the solution. To eliminate •HO from the reaction mixture, we modified the click reaction condition by adding 50% DMSO, a well-known •HO scavenger, into the reaction mixture. Under these conditions, no significant decomposition was observed, even for O-containing minicircles. Overall, the minicircles can be generated in 3 steps in 14-24%
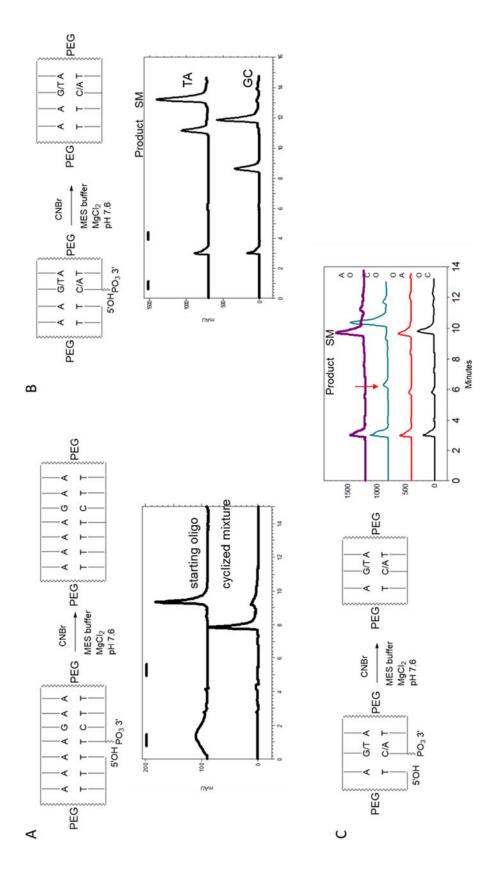
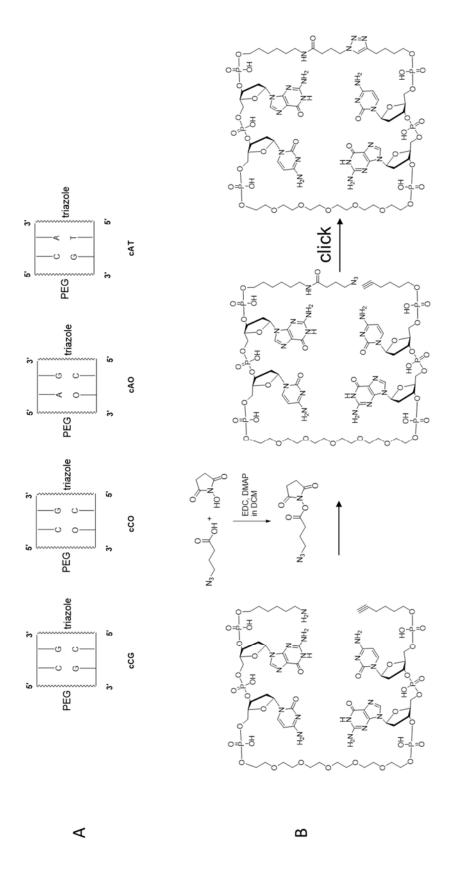**Figure 4.8** Ligation of nicked dumbbell DNA with CNBr.

Figure 4.9 Minicircle DNA. A) Sequences of minicircle DNA and B) synthetic approach.

yield.

The thermal stability of ligated minicircles was measured by monitoring the absorbance change with temperature at 260 nm. However, the hyperchromic change is too subtle even at high concentration, possibly due to minimal base stacking, to produce a cooperative transition. We thus resort to circular dichroism spectroscopy to monitor ellipticity changes of the long wavelength peak. A cooperative transition was observed for all minicircles. Not surprisingly, minicircle cCG is found to be quite stable as was reported previously (*32*). Replacing one of the G:C base pairs with an O:A or O:C base pair results in about 12-14 °C drop. Replacement with an A:T base pair further decreased the melting temperature another 16-18 °C. Thus, minicircles cCG, cCO, and cAO are stable enough for later TRIR study.

We also tried to elucidate the conformation of these minicircles at room temperature using CD spectra. Surprisingly, their room temperature CD spectra are wildly different (Figure 4.10). For minicircle cCG, we observed, consistent with Brown's data, a positive peak around 280 nm and a negative peak around 260 nm, indicating a B-form conformation is adopted by this minicircle DNA. The CD spectra of minicircle cCO is similar to that of cCG in overall shape. However, both the positive and negative peaks are red-shifted, indicating possible conformational deviation from a classical B-form structure. The red-shifted positive peak at 300 nm may be a combination of an overlapping positive signal associated with O above 300 nm (*vide infra*). Thus, the intrastrand base stacking in minicircle cCG and cCO are expected to be significant. It is well known that O can form a Hoogsteen base pair with A. The CD spectrum changes significantly when switching from the O:C to an O:A base pair in the minicircle cAO. The diagnostic negative peak at 290 nm and positive peak at 270 nm indicate a Z-form structure. For the Z-form, due to the
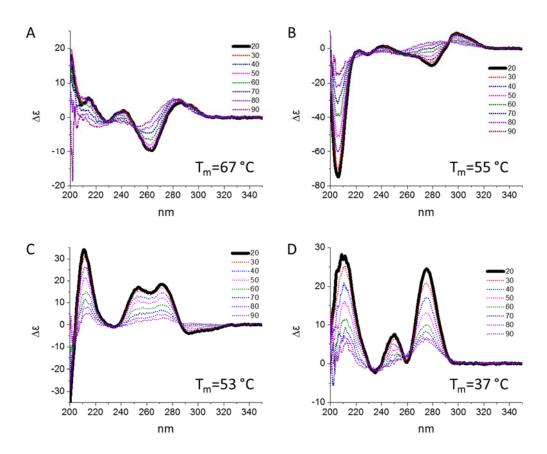
Figure 4.10 Circular dichroism change of minicircles (A: cCG; B: cCO; C: cAO; D: cAT;) at 20 °C (solid) and higher temperature (colored dots). Condition: 0.25 mM minicircles in 20 mM NaPi, 100 mM NaCl pH 7 buffer.

existence of a left-handed helix, the duplex exists in a zig-zag pattern which significantly disrupts intrastrand base stacking while promoting interstrand base stacking. However, we do not know whether base stacking exists between A and C bases or between O and G bases in the minicircle cAO. For minicircle cAT, we speculate it may adopt a B-form conformation as a positive peak was observed at 280 nm. Interestingly, all of the minicircles exhibited similar CD spectra when heated to 90 °C, at which temperature any secondary structures, base stacking, and pairing should have been destroyed.

Even though a hexaethylene glycol PEG linker has been previously shown to induce very little strain on the end of a DNA hairpin (*33*), its effect on a minicircle as short as two base pairs may be significant, leading to sequence-dependent structural variations. To further investigate if swapping base pairs could induce any further conformational change, we incorporated the minicircle unit into a hairpin structure and measured their CD spectra (Figure 4.11). In the UV absorption spectra of hairpins hpAO and hpCO, there are long wavelength tails above 300 nm which may originate from O as hpCG does not have this tail. The CD spectra of these three hairpins have very similar shapes. The negative peaks at 240 nm and 285 nm and positive peak at 260 nm are characteristic of an A-form conformation (*35*). The positive peaks above 300 nm only exist in O-containing hairpins, suggesting their origin from O. Irrespective of the *anti* or *syn* conformation of the O nucleobase adopted due to a different opposite base in the hairpins, only positive peaks above 300 nm are observed though the magnitude for hpAO is weaker. NMR (*35*), crystal structure (*36*), and molecular dynamics simulation (*35*) show all guanine bases stack very well in the dCCCCGGGG duplex while the stacking between cytosine bases is poor. Thus, it is expected that purine bases stack well in our hpGC and hpOC hairpins. However, it is
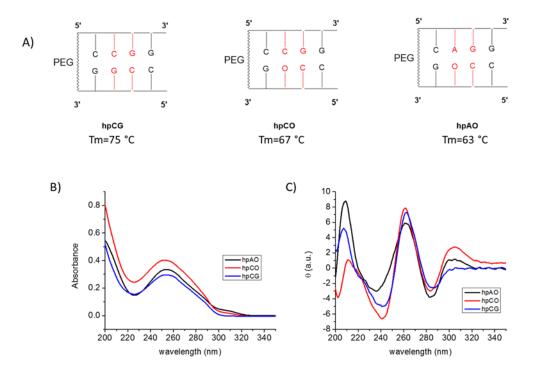
Figure 4.11 hpDNA. A) Sequences of hairpin and B) their UV and C) CD spectra using 50 mM DNA in 20 mM NaPi, 100 mM NaCl pH 7 buffer.

unclear how purine bases stack with their flanking bases in hpOA hairpin, especially the O:A base pair, due to the more disruption of consecutive purine and pyrimidine bases pattern.

It is well known that base stacking can affect the excited-state decay in dinucleotides and oligonucleotides (*23, 37*). Thus, it is necessary to further investigate the unique conformation adopted by O:A and O:C base pairs in these minicircles and hairpins to better understand the O excited-state decay in the following femtosecond transient-absorption experiment. By collaborating with a computational chemist (Anita Orendt, University of Utah), we will perform molecular dynamics simulation on these minicircles and hairpins to study how the base interacts with its flanking bases via base stacking and base pairing. The CD spectra will also be calculated using the TDDFT method and compared with experimental CD spectra to verify the simulated structures are consistent with the actual structures in the solution.

Irrespective of the molecular dynamics simulation study, we investigated the excited-state decay of the synthesized minicircles and hairpins. Preliminary results show strong IR signal bleaching likely originates from the carbonyl stretching for all bases in the mini circle molecules after the 265 nm excitation (Figure 4.12). This result is expected because, in the minicircle, all bases are interacting with each other via base stacking or base pairing interactions. To exclusively observe how the O excited-state decays in the minicircles, we selectively excited O using a 305 nm pump as other bases do not have absorbance at this wavelength. Due to base stacking and base pairing interactions with the O base, the bleaching signals originating from other bases should also be observed. Indeed, these bleaching signals can be detected except in minicircle cAO in which only the O signal is
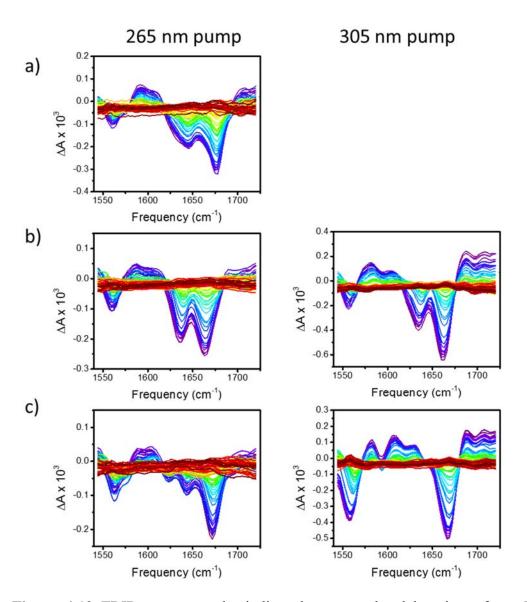
Figure 4.12 TRIR spectra at the indicated pump-probe delay times from 5 mM minicircles a) cCG, b) cCO, c) cAO solution in 20 mM NaPi, 100 mM NaCl pD 7 buffer.

detected (Figure 4.12). This unexpected result suggests O in the minicircle cAO does not stack well with other bases. Otherwise, the bleaching signal originating from other stacked bases should also be observed due to the decay of their CT state formation with O. This result also suggests minicircle cAO likely adopts a Z-form structure in which base A stacks with base C on the opposite strand. Nonetheless, we currently do not have a good explanation of why the bleaching signal from the opposite adenosine could not be observed considering it can interact with O via hydrogen bonding. Bleaching signals from hairpins could also be observed. However, due to the presence of intervening bases, we could not differentiate the signal. A detailed computational study and control experiments need to be done to further support the observed results and conclusions.

Conclusion

In this chapter, we studied the excited-state decay of O in various contexts using UV pump/Vis probe and UV pump/mid-IR probe techniques and learned that the excited-state decay is modulated by several factors including base stacking and base pairing. (Note: all experiments in ultrafast spectroscopy were performed at the Department of Chemistry and Biochemistry, Montana State University by Dr. Yuyuan Zhang.) Specifically, we found the decay of excited-state O nucleoside is dependent on its ionic state. Under neural conditions, it can quickly convert absorbed light energy into heat, which may explain its relative stability and wide occurrence in the genome. Under anionic conditions, however, it spends a longer time on its high energy state. This observation is consistent with its efficient ET repair of a thymine dimer.

We also optimized the synthesis of dinucleotide. This enables us to study the

synthesized dinucleotide using a sensitive UV-pump/mid-IR probe experiment. Using the base stacking in a dinucleotide as a minimal model of base stacking in dsDNA, we studied the effect of base stacking on electron transfer formation of the CT state and its decay. The significance of CT state formation between O and a neighboring base is two-fold. First, it provides a decay channel for the absorbed harmful light energy, which may explain why the DNA genome is relatively stable to UV irradiation. Second, it experimentally proves that O can repair thymine dimers in a photolyase-like manner. The relatively short lifetime of the CT state leads to a lower quantum yield of thymine dimer repair by O unless the back ET process is slow enough.

To better mimic a real system, we explored and developed a methodology to efficiently synthesize an O-containing minicircle structure in which O can both stack and pair with another base while keeping the structure as small as possible to simplify TRIR analysis. Preliminary results suggest the synthesized minicircle molecules adopt sequence-dependent conformations. The conformation may impact how the O excited-state decays. Further experiments need to be done to decipher how bases interact with each other in the minicircles and to differentiate the signal originating from each of the bases.

Experimental

All chemicals were purchased from commercial sources and used without further purification unless otherwise mentioned. The 5′-*O*-dimethoxytrityl-*N*-benzoyl-deoxyadenosine was purchased from Acros Organics, and 8-oxo-dG phosphoramidite and 2 M triethylammonium acetate (TEAA) were purchased from Glen Research. The 4,5-dicyanoimidazole and adamantane acetic acid were purchased from Alfa Aesar.

Dichloromethane (DCM) was freshly distilled. All other reagents and solvents were purchased from Aldrich and used without further purification.

Synthesis of d(OA) and d(AO)

Route 1: 3′-*O*-adamantane acetyl-5′-*O*-dimethoxytrityl-*N6*-benzoyl-deoxyadenosine (2). Commercially available 5′-*O*-dimethoxytrityl-*N6*-benzoyldeoxyadenosine **1** (100 mg), 1.5 equivalent adamantaneacetic acid, 1.6 equivalent 1-ethyl-3-(3-dimethylaminopropyl) carbodiimide, and 0.15 equivalent 4-dimethylaminopyridine were stirred in 2 mL dry DCM at room temperature for 2 h. After thin-layer chromatography (TLC) indicated reaction completion, the mixture was concentrated and taken up in EtOAc. The organic layer was washed with water, 10% (vol/vol) $KHSO_4$, water, saturated $NaHCO_3$, and brine. The organic layer was dried over $MgSO_4$, filtered, and concentrated. The residue was loaded onto silica gel [3% (vol/vol) Et_3N] and eluted with DCM:MeOH = 35:1, yielding 112.8 mg product **2** as white foam (yield 89%). High resolution mass spectrometry (HRMS), found for $[M+H]^+$: 834.3875 (calculated 834.3867). ^1H NMR (400 MHz, $CDCl_3$) δ 9.0 (br, 1H), 8.7 (s, 1H), 8.2 (s, 1H), 8.0 (d, J = 7.2 Hz, 2H), 7.6–7.5 (m, 3H), 7.4–7.2 (m, 9H), 6.7 (d, J = 9.2 Hz, 4H), 6.5 (t, J =8.2 Hz, 1H), 5.5 (m, 1H), 4.3 (m, 1H), 3.8 (s, 6H), 3.4 (s, 2H), 2.6–2.5 (m, 2H), 2.1 (s, 2H), 2.0–1.6 (m, 15H); ^{13}C NMR (100MHz, $CDCl_3$) δ 171.0, 158.6, 152.6, 151.5, 149.5, 144.4, 141.2, 135.5, 133.7, 132.8, 130.1, 130.0, 128.9, 128.1, 127.9, 127.8, 127.0, 123.3, 86.8, 84.7, 84.6, 74.7, 63.6, 55.2, 48.7, 42.5, 38.3, 36.7, 33.1, 28.6.

3′-*O*-adamantane acetyl-*N6*-benzoyl-deoxyadenosine (3). The 5′ tritylated and protected deoxyadenosine **2** (103 mg) was dissolved in DCM. Detritylation was achieved by using 2.1 equivalent triethylsilane and 5% (vol/vol) dichloroacetic acid within minutes.

DCM was added. The organic layer was washed with saturated Na_2CO_3, dried over $MgSO_4$, filtered, and concentrated. The crude material was loaded on silica gel and eluted with DCM:MeOH= 20:1 to afford 47.9 mg product **3** (yield 73%). HRMS found for [M+Na]+: 554.2380 (calculated 554.2377). ^{1}H NMR (400 MHz, CDCl$_3$) δ 9.0 (s, 1H), 8.8 (s, 1H), 8.1 (s, 1H), 8.0–7.5 (m, 5H) 6.3 (m, 1H), 5.7 (m, 1H), 5.6 (m, 1H), 4.4 (s, 1H), 4.0 (m, 2H), 3.2 (m, 1H), 2.5 (m, 1H), 2.1 (s, 2H), 2.0 (s, 3H), 1.7 (m, 12H); ^{13}C NMR (100 MHz, CDCl$_3$) δ 171.3, 164.5, 152.4, 150.9, 150.5, 142.6, 133.5, 133.1, 129.1, 128.0, 124.8, 88.1, 87.9, 75.9, 63.4, 48.8, 42.7, 38.0, 36.8, 33.2, 28.7.

d(OA) (4). Solution-phase synthesis of the dinucleotide d(OA) followed a related literature procedure (*24*). The procedure was modified as follows: 83.3 μmol of **3** and 100 μmol (1.2 equivalent) commercially available 8-oxo-dG phosphoramidite were mixed and coevaporated with ACN (3×). The mixture was dissolved in 0.7 mL ACN in an argon atmosphere. Dicyanoimidazole (300 μmol) was added. The mixture was stirred at room temperature until TLC showed the disappearance of the deoxyadenosine spot. I$_2$ (200 μmol) was added, and the mixture was stirred for 5 min. The reaction mixture was diluted with 30 mL ethyl acetate. Crude protected dinucleotide was extracted with 4 mL 0.5 M $Na_2S_2O_3$, 10% (vol/vol) $KHSO_4$, and then saturated $NaHCO_3$ and brine. The organic layer was dried with $MgSO_4$, filtered, and concentrated to produce a white foam. The crude product was dissolved in 1.9 mL acidic solution (0.1 M HCl prepared from ACN:MeOH = 2 mL:12 mL, and 0.1 mL acetyl chloride). After TLC showed complete removal of the dimethoxytrityl group, 1 mL 0.2 M TEAA was added. The partially deprotected dinucleotide was extracted with ethyl acetate. The organic layer was dried on $MgSO_4$, filtered, and concentrated to produce a white foam. The crude product was fully deprotected using 1 mL concentrated

NH$_3$ in the presence of 0.25 M 2-mercaptoethanol at 55 °C for 2 d. The mixture was concentrated and redissolved in water. The precipitate was removed, and the supernatant was purified on HPLC using ion exchange column and then C18 column to afford 21.5 μmol (yield 26%) white solid. The dinucleotide was characterized by HRMS [found for [M-H]$^-$ 595.1417 (calculated 595.1415)]. Analytical HPLC showed no difference between the dinucleotide obtained from the solution phase synthesis and the solid phase synthesis.

3'-*O*-adamantaneacetyl-5'-*O*-dimethoxytrityl-8-*Oxo*-*N*^{2}-isobutyryl-deoxygua-nosine (6) and 3'-*O*-adamantaneacetyl-*N*^{1}-adamantaneacetyl-5'-*O*-dimethoxy-trityl-8-oxo-*N*^{2}-isobutyryl-deoxyguanosine (7). Commercially available 5'-*O*-dimeth-oxytrityl-8-oxo-*N*^{2}-isobutyryl-deoxyguanosine **5** (100 mg), 3.5 equiv adamantaneacetic acid, 3.5 equiv 1-Ethyl-3-(3-dimethylaminopropyl)carbodiimide, and 0.15 equiv 4-Dimethylaminopyridine were stirred in 2 mL dry DCM at rt for 2 h. After TLC indicated reaction completion, the mixture was concentrated and taken up in EtOAc. The organic layer was washed with water, 10% KHSO$_4$, water, sat. NaHCO$_3$, and finally brine. The organic layer was dried over MgSO$_4$, filtrated, and concentrated. The residue was loaded onto silica gel (3% Et$_3$N) and eluted with a gradient of DCM:MeOH=50-35:1, yielding **6** and **7** (contaminated with adamantine acetic acid). **6**: ^{1}H NMR (400 MHz, CD$_2$Cl$_2$) δ 12.05 (br, 1H), 10.76 (br, 1H), 7.82 (s, 1H), 7.54 (m, 2H), 7.40 (m, 4H), 7.18-7.30 (m, 3H), 6.80 (m, 4H), 6.23 (dd, J=8.2, 6.0 Hz, 1H), 5.61 (ddd, J=6.4, 3.1, 2.9 Hz, 1 H), 4.08-4.14 (m, 1H), 3.77 (s, 3H), 3.76 (s, 3H), 3.41-3.53 (m, 2H), 3.14-3.22 (m, 1H), 2.25 (m, 1H), 2.08 (s, 2H), 1.95 (br, 3H), 1.61-1.74 (m, 12H), 0.97 (d, J=7.0 Hz, 3H), 0.72 (d, J=6.8 Hz, 3H); ^{13}C NMR (100 MHz, CD$_2$Cl$_2$) δ 178.6, 171.2, 158.7, 152.5, 150.0, 146.2, 145.3, 145.2, 136.5, 136.0, 130.0, 129.9, 128.1, 127.8, 126.9, 113.0, 104.8, 85.7, 83.3, 81.6, 74.0, 63.9,

55.1, 48.6, 42.3, 36.6, 35.9, 34.4, 32.8, 28.7, 18.4, 18.2.

3'-*O*-adamantaneacetyl-8-oxo-*N²*-isobutyryl-deoxyguanosine (8) and 3'-*O*-adamantaneacetyl-*N¹*-adamantaneacetyl-8-oxo-*N²*-isobutyryl-deoxyguanosine (9). 5' tritylated and protected deoxyguanosine **6** from the previous step was dissolved in DCM. Detritylation was achieved by 5%V dichloroacetic acid within minutes. DCM was added. The organic layer were washed with sat. Na_2CO_3, dried over $MgSO_4$, filtrated, and concentrated. The crude was loaded on silica gel and eluted with DCM:MeOH=20:1 to afford 16.3 mg product **8** (yield 20% over 2 steps). HRMS found for $[M+Na]^+$: 552.2435 (calcd 554.2434). ^1H NMR (400 MHz, CD_2Cl_2) δ 12.33 (br, 1H), 10.52 (br, 1H), 9.23 (br, 1H), 6.18 (dd, J=9.0, 5.9 Hz, 1 H), 5.30 (m, 1H), 4.58 (br, 1H), 4.07 (s, 1H), 3.75-3.86 (m, 2H), 3.01 - 3.08 (m, 1 H), 2.78 (quin, J=6.8 Hz, 1 H), 2.21 (dd, J=13.5, 6.1 Hz, 1 H), 2.09 (s, 2H), 1.98 (br, 3H), 1.62-1.75 (m, 12H), 1.32 (d, J=7.2 Hz, 3H), 1.28 (d, J=7.2 Hz, 3H); ^{13}C NMR (100 MHz, CD_2Cl_2) δ 179.4, 171.1, 152.0, 150.0, 147.3, 144.8, 104.4, 85.9, 82.8, 75.0, 63.0, 48.6, 42.3, 36.6, 36.3, 35.1, 32.9, 20.7, 18.7, 18.6.

The same procedure was used to remove DMT group and purify to afford 61.5 mg product **9** (yield 58% over 2 steps). HRMS found for $[M+Na]^+$: 728.3634 (calcd 728.3635). ^1H NMR (400 MHz, CD_2Cl_2) δ 11.99 (br, 1H), 8.92 (s, 1H), 6.22 (dd, J=9.2, 6.1 Hz, 1 H), 5.42 (m, 1 H), 4.12 (m, 1H), 3.85 - 3.89 (m, 2 H), 2.97-3.04 (m, 1H), 2.98 (d, J=14.4 Hz, 1H), 2.85 (d, J=14.4 Hz, 1H), 2.72 (m, 1 H), 2.26 (m, 1H), 2.11 (s, 2H), 1.97 (bs, 6H), 1.64-1.73 (m, 24H), 1.26 (d, J=5.2 Hz, 3H), 1.25 (d, J=5.2 Hz, 3H); ^{13}C NMR (100 MHz, CD_2Cl_2) δ 179.1, 171.2, 168.3, 150.0, 149.6, 149.0, 146.5, 102.7, 85.9, 83.0, 74.9, 63.1, 50.5, 48.5, 42.4, 42.3, 42.1, 36.7, 36.6, 36.3, 35.2, 34.2, 32.9, 28.8, 28.7, 28.7, 18.7, 18.5.

d(AO) (10). Solution phase synthesis of dinucleotide d(AO) followed a previous

procedure (*25*). The procedure was modified as follows. 85.2 μmol of **9** and 100 μmol (1.2 equiv) commercially available dA phosphoramidite were mixed and coevaporated with ACN (3X). The mixture was dissolved in 0.7 mL ACN in an argon atmosphere. Dicyanoimidazole (300 μmol) was added. The mixture was stirred at rt until TLC showed disappearance of the starting material spot. I_2 (200 μmol) was added, and the mixture was stirred for 5 min. The reaction mixture was diluted with 30 mL ethyl acetate. Crude protected dinucleotide was extracted with 4 mL 0.5 M $Na_2S_2O_3$, 10% $KHSO_4$, sat. $NaHCO_3$, brine. The organic layer was dried on $MgSO_4$, filtered, and concentrated to give a white foam. The crude mixture was dissolved in 1.9 mL acidic solution (0.1 M HCl prepared from ACN:MeOH=2 mL:12 mL, and 0.1 mL acetyl chloride). After TLC showed complete removal of the DMT group, 1 mL 0.2 M TEAA was added. The partially deprotected dinucleotide was extracted with ethyl acetate. The organic layer was dried on $MgSO_4$, filtered, and concentrated to give a white foam. The crude product was fully deprotected using 1 mL conc. NH_3 in the presence of 0.25 M 2-mercaptoethanol at 55 °C for 2 days. The mixture was concentrated and redissolved in water. The precipitate was removed, and the supernatant was purified on HPLC using C18 column to afford 15.3 μmol (yield 18%) white solid. The dinucleotide was characterized by HRMS [found for [M-H]⁻: 595.1425 (calcd 595.1415)].

Route 2: The protocol for solid-phase synthesis was modified as follows. Two 15 μmol support containing prepacked column was soaked with acetonitrile. DMT group was cleaved using 3% DCA in DCM for 2 min. The columns were repeatedly washed with acetonitrile for 6 times or 3 more times after the color disappearance. Next, the free hydroxyl group was reacted with 50 μmol phosphoramidite in 1 mL dry acetonitrile and

250 μmol DCI in 1 mL acetonitrile for 40 min at room temperature. The columns were washed again after the reaction using acetonitrile. The newly formed phosphite group was oxidized using 0.02 M I_2 in THF/Pyridine/H_2O for 2 min. The columns were again repeatedly washed with acetonitrile for 6 times or 3 more times after the color disappearance. The DMT group was cleaved again using 3% DCA in DCM for 2 min. The dinucleotide was cleaved and deprotected using concentrated ammonium hydroxide. It was then purified using above-mentioned methods in 40~50% yield.

Synthesis of minicircle

Route 1: minicircle with double PEG linkers. 3' Phosphorylated oligonucleotides were synthesized using standard phosphoramidite chemistry and purified at the University of Utah DNA-Peptide Core Facility. The ligation was achieved using a modified literature method (*38*). Nicked dumbbell oligonucleotide (0.1 mM) in 20 mM $MgCl_2$, 250 mM MES pH 7.6 buffer was annealed and kept at 0 °C at least 15 min before adding 100 μL 5 M CNBr acetonitrile solution. The mixture was allowed to stand at 0 °C for 5 min; then 1 mL 2% $LiClO_4$ acetone solution was added to precipitate oligomer. To maximize the recovery of oligomer from the solution, the solution was incubated on dry ice for at least 30 min, violently vortexed until solid appeared. The solid was recovered by 10 min centrifugation at 10, 000 rpm. The pellet was washed once with cold acetone, dried down, redissolved in water, and analyzed on HPLC using a reverse phase column.

Route 2: minicircle with PEG and triazole linkers. 5'-Alkyne modified oligonucleotides were synthesized on multiples of 1 μmol scale using standard phosphoramidite chemistry at the University of Utah DNA-Peptide Core Facility. The oligonucleotides were cleaved

from the solid support and deprotected by incubating in concentrated NH_3 with 0.25 M 2-mercaptoethanol at 55°C for 24 h. The oligo was purified by HPLC on a reversed-phase column in which mobile phase A= 20 mM ammonium acetate, pH 7 and B=acetonitrile running a gradient from 7-20% B in 30 min at 1 mL/min by monitoring the absorbance at 260 nm. A 3'-azide was attached by adding excess 4-azidobutyrate NHS ester to the purified oligonucleotides from the last step in acetonitrile/0.5 M $NaHCO_3$ buffer at pH 8.7. The mixture was incubated at room temperature overnight. The crude azide-conjugated oligonucleotide was purified using the same method as before.

The oligonucleotides were cyclized by employing the following modified method (*32*). 200 μM DNA, 0.2 M triethylammonium acetate buffer (from 2 M stock, pH 7), 55 vol% DMSO, and 0.5 mM fresh ascorbic acid were mixed well in an Eppendorf tube. The solution was degassed by bubbling inert gas for 1 min. Then 0.5 mM Cu(II)-TBTA complex (from 10 mM stock in 55 vol% DMSO) was added. The tube was capped and allowed to sit at room temperature overnight. The clicked oligonucleotides mixture was desalted on a NAP column and purified by RP-HPLC using the same method as before.

Thermal stability study of minicircles and hairpins. Circular dichroism spectra were obtained using a JASCO J-815 spectrometer for aqueous solutions of 0.25 mM minicurcles (0.05 mM hairpins) in 20 mM NaPi, 100 mM NaCl pH 7 buffer to give sufficient signal-to-noise ratio. The melting curve was obtained by measuring the change in absorbance at 260 nm from 20 °C to 90 °C at a heating ramp rate of 0.5 °C/min. The melting temperature of hairpins were obtained using a Shimadzu UV-1800 UV-VIS spectrophotometer by measuring absorbance change at 260 nm of 8 μM hairpin in 20 mM NaPi, 100 mM NaCl

pH 7 buffer from 80 °C to 20 °C at a rate of 1 °C/min. The melting temperature was found using first derivative method.

References

1.   Woese, C. R. (1967) *The genetic code*, Harper and Row, New York.

2.   Crick, F. H. (1968) The origin of the genetic code, *J. Mol. Biol. 38*, 367-379.

3.   Orgel, L. E. (1968) Evolution of the genetic apparatus, *J. Mol. Biol. 38*, 381-393.

4.   Gilbert, W. (1986) Origin of life: The RNA world, *Nature 319*, 618-618.

5.   Ban, N., Nissen, P., Hansen, J., Moore, P. B., and Steitz, T. A. (2000) The complete atomic structure of the large ribosomal subunit at 2.4 A resolution, *Science 289*, 905-920.

6.   Wimberly, B. T., Brodersen, D. E., Clemons, W. M., Jr., Morgan-Warren, R. J., Carter, A. P., Vonrhein, C., Hartsch, T., and Ramakrishnan, V. (2000) Structure of the 30S ribosomal subunit, *Nature 407*, 327-339.

7.   Yusupov, M. M., Yusupova, G. Z., Baucom, A., Lieberman, K., Earnest, T. N., Cate, J. H., and Noller, H. F. (2001) Crystal structure of the ribosome at 5.5 A resolution, *Science 292*, 883-896.

8.   White, H. B., 3rd. (1976) Coenzymes as fossils of an earlier metabolic state, *J. Mol. Evol. 7*, 101-104.

9.   Tsukiji, S., Pattnaik, S. B., and Suga, H. (2003) An alcohol dehydrogenase ribozyme, *Nat. Struct. Biol. 10*, 713-717.

10.   Tsukiji, S., Pattnaik, S. B., and Suga, H. (2004) Reduction of an aldehyde by a NADH/Zn^{2+} -dependent redox active ribozyme, *J. Am. Chem. Soc. 126*, 5044-5045.

11.   Powner, M. W., Gerland, B., and Sutherland, J. D. (2009) Synthesis of activated pyrimidine ribonucleotides in prebiotically plausible conditions, *Nature 459*, 239-242.

12.   Powner, M. W., Sutherland, J. D., and Szostak, J. W. (2010) Chemoselective multicomponent one-pot assembly of purine precursors in water, *J. Am. Chem. Soc. 132*, 16677-16688.

13.   Nguyen, K. V., and Burrows, C. J. (2011) A prebiotic role for 8-oxoguanosine as a flavin mimic in pyrimidine dimer photorepair, *J. Am. Chem. Soc. 133*, 14586-14589.

14.   Nguyen, K. V., and Burrows, C. J. (2012) Photorepair of cyclobutane pyrimidine dimers by 8-oxopurine nucleosides, *J. Phys. Org. Chem. 25*, 574-577.

15. Nguyen, K. V., and Burrows, C. J. (2012) Whence flavins? Redox-active ribonucleotides link metabolism and genome repair to the RNA world, *Acc. Chem. Res. 45*, 2151-2159.

16. Kumar, A., and Sevilla, M. D. (2013) Excited state proton-coupled electron transfer in 8-oxoG-C and 8-oxoG-A base pairs: a time dependent density functional theory (TD-DFT) study, *Photochem. Photobiol. Sci. 12*, 1328-1340.

17. Middleton, C. T., de La Harpe, K., Su, C., Law, Y. K., Crespo-Hernandez, C. E., and Kohler, B. (2009) DNA excited-state dynamics: from single bases to the double helix, *Annu. Rev. Phys. Chem. 60*, 217-239.

18. Pecourt, J. M., Peon, J., and Kohler, B. (2001) DNA excited-state dynamics: ultrafast internal conversion and vibrational cooling in a series of nucleosides, *J. Am. Chem. Soc. 123*, 10370-10378.

19. Rios, A. C., and Tor, Y. (2013) On the origin of the canonical nucleobases: an assessment of selection pressures across chemical and early biological evolution, *Isr. J. Chem. 53*, 469-483.

20. Fleming, A. M., Muller, J. G., Dlouhy, A. C., and Burrows, C. J. (2012) Structural context effects in the oxidation of 8-oxo-7,8-dihydro-2'-deoxyguanosine to hydantoin products: electrostatics, base stacking, and base pairing, *J. Am. Chem. Soc. 134*, 15091-15102.

21. Luo, W., Muller, J. G., and Burrows, C. J. (2001) The pH-dependent role of superoxide in riboflavin-catalyzed photooxidation of 8-oxo-7,8-dihydroguanosine, *Org. Lett. 3*, 2801-2804.

22. Zhang, Y., Dood, J., Beckstead, A., Chen, J., Li, X. B., Burrows, C. J., Lu, Z., Matsika, S., and Kohler, B. (2013) Ultrafast excited-state dynamics and vibrational cooling of 8-oxo-7,8-dihydro-2'-deoxyguanosine in D2O, *J. Phys. Chem. A 117*, 12851-12857.

23. Takaya, T., Su, C., de La Harpe, K., Crespo-Hernandez, C. E., and Kohler, B. (2008) UV excitation of single DNA and RNA strands produces high yields of exciplex states between two stacked bases, *Proc. Natl. Acad. Sci. U.S.A. 105*, 10285-10290.

24. de Koning, M. C., Ghisaidoobe, A. B. T., Duynstee, H. I., Ten Kortenaar, P. B. W., Filippov, D. V., and van der Marel, G. A. (2006) Simple and Efficient Solution-Phase Synthesis of Oligonucleotides Using Extractive Work-Up, *Org. Process. Res. Dev. 10*, 1238-1245.

25. Zhang, Y., Dood, J., Beckstead, A. A., Li, X. B., Nguyen, K. V., Burrows, C. J., Improta, R., and Kohler, B. (2014) Efficient UV-induced charge separation and

recombination in an 8-oxoguanine-containing dinucleotide, *Proc. Natl. Acad. Sci. U.S.A. 111*, 11612-11617.

26. Zhang, Y., Dood, J., Beckstead, A. A., Li, X.-B., Nguyen, K. V., Burrows, C. J., Improta, R., and Kohler, B. (2015) Photoinduced Electron Transfer in DNA: Charge Shift Dynamics Between 8-Oxo-Guanine Anion and Adenine, *J. Phys. Chem. B*, ASAP, DOI: 10.1021/jp511220x.

27. Liu, Z., Tan, C., Guo, X., Kao, Y. T., Li, J., Wang, L., Sancar, A., and Zhong, D. (2011) Dynamics and mechanism of cyclobutane pyrimidine dimer repair by DNA photolyase, *Proc. Natl. Acad. Sci. U.S.A. 108*, 14831-14836.

28. Kao, Y. T., Song, Q. H., Saxena, C., Wang, L., and Zhong, D. (2012) Dynamics and mechanism of DNA repair in a biomimetic system: flavin-thymine dimer adduct, *J. Am. Chem. Soc. 134*, 1501-1503.

29. O'Neill, M. A., and Barton, J. K. (2002) Effects of strand and directional asymmetry on base-base coupling and charge transfer in double-helical DNA, *Proc. Natl. Acad. Sci. U.S.A. 99*, 16543-16550.

30. Bucher, D. B., Schlueter, A., Carell, T., and Zinth, W. (2014) Watson-crick base pairing controls excited-state decay in natural DNA, *Angew. Chem. Int. Ed. 53*, 11366-11369.

31. Banyay, M., Sarkar, M., and Graslund, A. (2003) A library of IR bands of nucleic acids in solution, *Biophys. Chem. 104*, 477-488.

32. El-Sagheer, A. H., Kumar, R., Findlow, S., Werner, J. M., Lane, A. N., and Brown, T. (2008) A very stable cyclic DNA miniduplex with just two base pairs, *Chembiochem 9*, 50-52.

33. McCullagh, M., Zhang, L., Karaba, A. H., Zhu, H., Schatz, G. C., and Lewis, F. D. (2008) Effect of loop distortion on the stability and structural dynamics of DNA hairpin and dumbbell conjugates, *J. Phys. Chem. B 112*, 11415-11421.

34. Merenkova, I. P., Dolinnaia, N. G., Oretskaia, T. S., Sokolova, N. I., and Shabarova, Z. A. (1992) Chemical reactions in double-helical nucleic acids. XIV. Effectiveness of forming phosphodiester bonds between various nucleotide units, *Bioorg. Khim. 18*, 85-91.

35. Trantirek, L., Stefl, R., Vorlickova, M., Koca, J., Sklenar, V., and Kypr, J. (2000) An A-type double helix of DNA having B-type puckering of the deoxyribose rings, *J. Mol. Biol. 297*, 907-922.

36. Haran, T. E., Shakked, Z., Wang, A. H., and Rich, A. (1987) The crystal structure of d(CCCCGGGG): a new A-form variant with an extended backbone conformation, *J. Biomol. Struct. Dyn. 5*, 199-217.

37. Chen, J., and Kohler, B. (2014) Base stacking in adenosine dimers revealed by femtosecond transient absorption spectroscopy, *J. Am. Chem. Soc. 136*, 6362-6372.

38. Carriero, S., and Damha, M. J. (2003) Synthesis of lariat-DNA via the chemical ligation of a dumbbell complex, *Org. Lett. 5*, 273-276.

CHAPTER 5

FUTURE WORK

Even though the redox potentials of 5-hydroxypyrimidine bases are similar to that of
O (*1*), their thymine dimer repair ability in ssDNA and dsDNA context is remarkably
different. Pyrimidine bases generally have low propensity of base stacking with other bases.
Thus, the poor base stacking ability of 5-hydroxypyrimidines may contribute to their low
thymine dimer repair ability. To exclude the base stacking factor, we compared 5-
hydroxypyrimidine nucleosides and O nucleosides' thymine dimer repair ability.
Preliminary results show that the repair ability of 5-hydroxypyrimidine nucleosides are
also low compared to O nucleoside. Noticeably, there is no observed pH effect on thymine
dimer repair rate in 5-hydroxypyrimidine catalyzed reactions (Figure 5.1). The lack of
elevated repair rate at high pH at which the electron transfer rate is thought to be faster
suggests a short excited-state lifetime of 5-hydroxypyrimidine may account for the
observed result. A longer excited-state lifetime was previously proposed (*2*) and later
confirmed as shown in Chapter 4 and ref (*3*) to account for the observed higher thymine
dimer repair rate at high pH by an O nucleoside. To verify this hypothesis, the excited-state
lifetime of 5-hydroxypyrimidine in the neutral and anionic states should be measured in a
UV-pump/mid-IR-probe experiment. In the oligonucleotide context, the pH effect on
thymine dimer repair by 5-hydroxycytosine (5-HC) was observed while no pH effect was
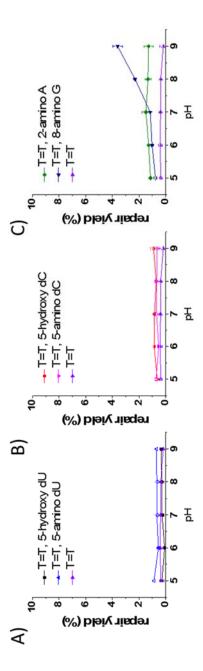
Figure 5.1 pH effect on photo-induced thymine dimer repair by modified nucleosides. Reaction condition: same as ref. (*2*).

observed by the O mediated reaction. Thus, we will also measure the excited-state lifetime of a 5-HC-containing dinucleotide to investigate the base stacking effect. The optimized dinucleotide synthesis methodology, as was delineated in Chapter 4, can also be used to efficiently synthesize a 5-HC-containing dinucleotide.

Initially dinucleotides were synthesized using a modified solution-phase synthesis method (*4*) in which a key hydrophobic group was installed to facilitate the late stage liquid-liquid extraction. However, the recovery yield for this procedure can be very low, possibly due to premature cleavage of the labile protecting group on the phosphate group during the extraction procedure. Other drawbacks for this methodology are the lengthy preparation steps for starting materials which can increase the preparation time and cost. The turnaround time for this methodology is about 3 weeks. Thus, we resorted to a solid-phase synthesis method. Compared to the solution-phase synthesis method, the turnaround time for this method is short, and the yield is high. However, it may also be expensive especially if a costly modified phosphoramidite is needed because the DNA auto-synthesizer usually delivers a large excess of phosphoramidite to achieve >99% coupling yield. Accordingly, we modified the solid-phase synthesis procedure, especially the coupling step. Instead of using the synthesizer to do the coupling, we performed manual coupling in which only a 3-fold excess of phosphoramidite was needed. The turnaround time for manual solid phase synthesis is as short as automatic solid-phase synthesis. The major advantage is that it can cut the cost.

In photolyase, flavin-mediated electron transfer (ET) repair of a thymine dimer can achieve close to unity quantum yield (*5*). However, in a flavin-CPD model system, the quantum yield scores only at 0.05 (*6*). The extremely low quantum yield was previously

(ref. Chapter 1) proposed to be determined by two factors: (1) a long excited-state lifetime of flavin (1.3 ns) vs. fast forward electron transfer (ET) to thymine dimer (250 ps); (2) slow futile back ET from the thymine dimer radical anion to flavin radical (2.4 ns) vs. fast second bond C_6-$C_{6'}$ cleavage (90 ps). In the best case of an O-containing dsDNA, the repair quantum yield can only achieve up to 0.01. To investigate which steps contribute to the low quantum yield in our system, we will try to map out the time constant for each step of thymine dimer repair in a designed model oligonucleotide, dOT=T. Using the optimized dinucleotide synthesis methodology, we can make this trinucleotide, dOT=T, much cheaply than originally thought.

References

1.   Yanagawa, H., Ogawa, Y., and Ueno, M. (1992) Redox ribonucleosides. Isolation and characterization of 5-hydroxyuridine, 8-hydroxyguanosine, and 8-hydroxyadenosine from Torula yeast RNA, *J. Biol. Chem. 267*, 13320-13326.

2.   Nguyen, K. V., and Burrows, C. J. (2012) Photorepair of cyclobutane pyrimidine dimers by 8-oxopurine nucleosides, *J. Phys. Org. Chem. 25*, 574-577.

3.   Zhang, Y., Dood, J., Beckstead, A., Chen, J., Li, X. B., Burrows, C. J., Lu, Z., Matsika, S., and Kohler, B. (2013) Ultrafast excited-state dynamics and vibrational cooling of 8-oxo-7,8-dihydro-2'-deoxyguanosine in D2O, *J. Phys. Chem. A 117*, 12851-12857.

4.   de Koning, M. C., Ghisaidoobe, A. B. T., Duynstee, H. I., Ten Kortenaar, P. B. W., Filippov, D. V., and van der Marel, G. A. (2006) Simple and Efficient Solution-Phase Synthesis of Oligonucleotides Using Extractive Work-Up, *Org. Process. Res. Dev. 10*, 1238-1245.

5.   Liu, Z., Tan, C., Guo, X., Kao, Y. T., Li, J., Wang, L., Sancar, A., and Zhong, D. (2011) Dynamics and mechanism of cyclobutane pyrimidine dimer repair by DNA photolyase, *Proc. Natl. Acad. Sci. U.S.A. 108*, 14831-14836.

6.   Song, Q.-H., Tang, W.-J., Ji, X.-B., Wang, H.-B., and Guo, Q.-X. (2007) Do Photolyases Need To Provide Considerable Activation Energy for the Splitting of Cyclobutane Pyrimidine Dimer Radical Anions?, *Chem. Eur. J. 13*, 7762-7770.